

EQUIVALENT CIRCUIT MODEL GENERATION FOR BATTERIES USING
NON-IDEAL TEST DATA

by

Logan Crain

A Thesis Submitted in

Partial Fulfillment of the

Requirements of the Degree of

Master of Science

in Engineering

at

The University of Wisconsin-Milwaukee

December 2018

ABSTRACT

EQUIVALENT CIRCUIT MODEL GENERATION FOR BATTERIES USING NON-IDEAL TEST DATA

by

Logan Crain

The University of Wisconsin-Milwaukee, 2018
Under the Supervision of Professor Deyang Qu

Modeling is a key component in the development of battery products. While there are multiple levels of complexity which may be achieved in model development, equivalent circuit modeling is able to quickly produce reliable and accurate predictions for battery behavior. Though the use of equivalent circuit models has been described in great detail for lithium ion batteries, it is also desirable to use this methodology regardless of chemistry, specifically with respect to lead-acid technology. When developing battery models for predicting battery behavior in a vehicle, the testing methods meant to mimic vehicle applications often cause non-ideal data for model generation. Specifically, periods of constant voltage charging can limit the model's robustness and accuracy. This is due to the imposed voltage limit required for constant voltage charging which is not an inherent battery behavior. By thoroughly examining equivalent circuit models of increasing complexity, it is shown that lead-acid and lithium ion batteries behave similarly so that minimal impact is had on model development. Additionally, three methods are considered for modifying the fitting process so that test data which contains voltage limits may still be considered useful for model development.

© Copyright by Logan Crain, 2018
All Rights Reserved

TABLE OF CONTENTS

LIST OF FIGURES.....	vi
LIST OF TABLES.....	ix
ACKNOWLEDGEMENTS	xi
1. Introduction	1
2. Background.....	4
2.1 Battery Testing.....	4
2.1.1 Open Circuit Voltage testing.....	4
2.1.2 Capacity Testing	5
2.1.3 Additional Testing.....	5
2.1.4 Voltage Limits & Testing	8
2.2 Battery Modeling.....	9
2.2.1 Model Selection.....	9
2.2.2 Equivalent Circuit Modeling.....	10
2.2.3 Discretization of Model Equations	13
2.2.4 Initial Guess Determination for Model Parameters.....	14
2.3 Model Verification	16
3. Generation and Comparison of Equivalent Circuit Models.....	19
3.1 Lithium Ion Modeling.....	19
3.1.1 Internal Resistance Model.....	21
3.1.2 Thevenin Battery Model	22
3.1.3 Modified Thevenin Battery Model.....	24
3.1.4 Lithium Ion Fitting Summary.....	26
3.2 Lead Acid Modeling	28
3.2.1 Internal Resistance Model.....	30
3.2.2 Thevenin Battery Model	31
3.2.3 Modified Thevenin Battery Model.....	32
3.2.4 Lead Acid Fitting Summary	34

3.3 Conclusion	34
4. Voltage Limit Impact on Fitting Method	36
4.1 Baseline Case – No Modification	37
4.2 Window Skip Algorithm	39
4.3 Secondary Constant Voltage ECM	41
4.4 Conclusion	46
5. Conclusion	47
REFERENCES.....	49

LIST OF FIGURES

Figure 1: Example of low load power profile for worldwide harmonized light vehicle testing procedure (WLTP) 6

Figure 2: Zoomed in look at high power level HPPC pulse @ 25C for lithium ion cell 7

Figure 3: Internal Resistance Equivalent Circuit Model schematic..... 11

Figure 4: Thevenin Equivalent Circuit Model schematic..... 12

Figure 5: Initial guess parameter extraction. R0 taken from initial 10 ms of pulse, R1 taken from final voltage of pulse, C1 taken from relaxation after the pulse 15

Figure 6: Representation of model implementation to predict performance given an input power profile 18

Figure 7: SOC vs. OCV relationship for lithium ion battery used in HPPC testing..... 20

Figure 8: (a) Internal Resistance model comparison of predicted voltage vs. measured test voltage, (b) Measured test current..... 21

Figure 9: Internal resistance model behavior for lithium ion HPPC testing (a) Predicted vs. measured voltage in moderate low current discharge pulse, (b) Measured current for pulse in (a), (c) Predicted vs. measured voltage in moderate low current charge pulse, (d) Measured current in (c)..... 22

Figure 10: Thevenin model behavior for lithium ion HPPC testing (a) Predicted vs. measured voltage in moderate low current discharge pulse, (b) Measured current for pulse in (a), (c) Predicted vs. measured voltage in moderate low current charge pulse, (d) Measured current in (c)..... 23

Figure 11: (a) Modified Thevenin model comparison of predicted voltage vs. measured test voltage, (b) Measured test current..... 24

Figure 12: Modified Thevenin model behavior for lithium ion HPPC testing (a) Predicted vs. measured voltage in moderate high current discharge pulse, (b) Measured current for pulse in (a), (c) Predicted vs. measured voltage in moderate high current charge pulse, (d) Measured current in (c) 25

Figure 13: Thevenin model behavior for lithium ion HPPC testing when fitting for only the low current pulses (a) Predicted vs. measured voltage in low current discharge pulse, (b) Measured current for pulse in (a), (c) Predicted vs. measured voltage in low current charge pulse, (d) Measured current in (c) 27

Figure 14: SOC vs. OCV relationship for lead acid battery used in WLTP testing 29

Figure 15: (a) Internal Resistance model comparison of predicted voltage vs. measured test voltage, (b) Measured test current..... 30

Figure 16: (a) Thevenin model comparison of predicted voltage vs. measured test voltage, (b) Measured test current 31

Figure 17: Modified Thevenin model comparison of predicted voltage vs. measured test voltage, (b) Measured test current 33

Figure 18: Baseline case fitting method for Modified Thevenin ECM of high load WLTP power profile (a) Measured vs. predicted power, (b) Instantaneous, absolute error in power, (c) SOC calculated from test vs. modeled SOC..... 37

Figure 19: Baseline case fitting method for Modified Thevenin ECM of high load WLTP power profile (a) Measured vs. modeled voltage, (b) Measured vs. modeled current ... 38

Figure 20: Window skip algorithm fitting method for Modified Thevenin ECM of high load WLTP power profile (a) Measured vs. predicted power, (b) Instantaneous, absolute error in power, (c) SOC calculated from test vs. modeled SOC 39

Figure 21: Window skip algorithm fitting method for Modified Thevenin ECM of high load WLTP power profile (a) Measured vs. modeled voltage, (b) Measured vs. modeled current 40

Figure 22: Modification of Figure 6. to include secondary ECM when the battery is in a state of constant voltage charging. Branches indicate a return to Figure 6. 43

Figure 23: Secondary constant voltage ECM fitting method for Modified Thevenin ECM of high load WLTP power profile (a) Measured vs. predicted power, (b) Instantaneous, absolute error in power, (c) SOC calculated from test vs. modeled SOC 44

Figure 24: Secondary constant voltage ECM fitting method for Modified Thevenin ECM of high load WLTP power profile (a) Measured vs. modeled voltage, (b) Measured vs. modeled current 45

LIST OF TABLES

Table 1: Voltage limits used in testing of lead acid and lithium ion batteries	8
Table 2: Battery model classifications and trade offs.....	10
Table 3: Mutli-current description for charge and discharge at 80% SOC in HPPC testing.....	19
Table 4: Summary of accuracy for the internal resistance ECM prediction of lithium ion voltage in HPPC testing	22
Table 5: Summary of accuracy for the Thevenin ECM prediction of lithium ion voltage in HPPC testing.....	24
Table 6: Summary of accuracy for the Modified Thevenin ECM prediction of lithium ion voltage in HPPC testing	25
Table 7: Summary of accuracy for each model considered in lithium ion HPPC testing	26
Table 8: Summary of accuracy for the Internal Resistance ECM prediction of lead acid voltage in WLTP testing	31
Table 9: Summary of accuracy for the Thevenin ECM prediction of lead acid voltage in WLTP testing.....	32
Table 10: Summary of accuracy for the Modified Thevenin ECM prediction of lead acid voltage in WLTP testing	33
Table 11: Summary of accuracy for each model considered in lead acid WLTP testing	34
Table 12: Summary of prediction accuracy for baseline fitting method of high load WLTP power profile using the Modified Thevenin ECM	38

Table 13: Summary of prediction accuracy for window skip algorithm fitting method of high load WLTP power profile using the Modified Thevenin ECM..... 41

Table 14: Summary of prediction accuracy for secondary constant voltage ECM fitting method of high load WLTP power profile using the Modified Thevenin ECM..... 45

ACKNOWLEDGEMENTS

I would first like to thank my advisor Prof. Deyang Qu for all of his guidance and support in determining my path within UWM. Many times in the last few years he was able to provide me with an idea or a solution to the problems I came across. His knowledge and advice has also been very beneficial for my professional career. I also want to thank Professor Ilya Avdeev for being on my thesis defense committee.

Secondly, I would like to extend a thank you to Johnson Controls for providing me the opportunity to pursue my MS and continue my studies. Specifically, I would like to thank my boss Zoe Jin for her continued help and guidance and for acting as a second advisor and mentor for me throughout the entirety of the process. I would also like to thank the modeling team for supporting my work.

I would like to thank my family for their love, support, and guidance throughout my life.

Lastly, I would like to thank my fiancé. She has been incredibly supportive of my work and I would not have been able to do this without her.

1. Introduction

As climate change becomes an increasing concern, the fuel efficiency of vehicles is receiving a higher level of scrutiny.^[1] With this comes an increased reliance on battery performance to sustain the electrification of vehicles. Regardless of whether the vehicle is fully electric or relies on an internal combustion engine, the battery is being tasked with a higher level of responsibility.^[2,3] Newer battery-vehicle applications such as regenerative braking and start-stop are able to improve fuel efficiency through strategic leverage of either the lead acid or lithium ion batteries in their powertrain.

To meet the growing demand in battery performance, it is imperative to develop battery models to accurately assess various designs. Modeling provides a low cost accelerated alternative to testing. Additionally, it allows for large scale analysis which would be cost prohibitive in a testing environment. The model is selected according to its accuracy in predicting battery behavior including peak power performance and energy throughput as well as its ease of implementation.

Choosing a model which delivers the highest accuracy while limiting the time for development and implementation requires a careful balancing. Physical based models which deliver the highest level of accuracy also require the greatest number of input variables and place the most emphasis on computing power and time. Statistical models require a large sample size and may have hidden bias which cannot be assessed depending on data collection methods. Therefore, in industry it is important to find some type of model which has high accuracy with limited parameters and quick implementation.

Fortunately, equivalent circuit models (ECM) were developed to achieve this goal.^[4,5]

By transforming the complex electrochemistry of a battery into a simple circuit, ECMs reduce the number of parameters to a minimum. Additionally, they require a low level of complexity and can be solved with a simpler discretization method when compared to full scale physical models.

Due to the maturity of ECMs, there are ranging levels of complexity developed to describe a large range in battery behaviors.^[6-10] The simplest ECM combines a voltage source with a resistor meant to mimic the battery's open circuit voltage and internal resistance. This model is capable of predicting the initial battery response, but does not provide insight into the polarization of the battery during and after a charge or discharge. Improvements can be made by adding a resistor and capacitor (RC block, in parallel with one another) in series with the primary resistor commonly referred to as the Thevenin ECM. For the highest level of accuracy, multiple RC blocks may be placed in series. Additionally, the model can be transformed into an impedance model when considering an infinite number of RC blocks.^[11,12] While these models offer higher levels of accuracy, they also require additional testing and circuit elements which need to be determined.

Within industry it is common to use either a one or two block RC ECM. This requires minimal parameters while still capturing some dynamic behavior of the battery – which is important for modeling vehicle applications. However, a one block RC model provides near the same accuracy as the two block RC model so that it may typically be deemed sufficient.^[10]

Though research has been conducted on lead-acid battery ECM's, their primary function appears to be within lithium ion battery modeling. Lead-acid batteries remain an integral component to vehicles even in the increasingly electrified environment. Therefore, it is necessary to understand the limitations in using the same approach towards lead acid battery modeling as lithium ion modeling.

The behavior of ECMs is well described within research (as previously noted) in areas where the battery is not inhibited by the testing or vehicle controls. However, there is little to no available work which relays how these models perform otherwise. Often when a battery is in a vehicle, it is subjected to periods of constant voltage – also known as voltage limits. These limits alter the battery response and lead to inaccurate predictions when using models that do not account for them. Therefore, it is the goal of this thesis to describe ECM behavior in voltage limited regions which may result from testing at high loads or with the purpose of mimicking vehicle behavior. The second goal is to determine how accuracy may be improved for this type of modeling in both lead acid and lithium ion batteries.

2. Background

In battery modeling, there are three key areas which contribute to the model generation: battery testing, model selection, and the model validation. The following section provides some background and overview on these three areas as they relate to the following discussion.

2.1 Battery Testing

In order to develop the model, multiple characterization tests are required. The number of tests which are needed depends on the complexity of the model. Ideally, the tests are selected with model development in mind, however this is not always the case. This test data can provide challenges as will be discussed later. All tests used in this thesis' model development are outlined and explained below.

2.1.1 Open Circuit Voltage testing

A battery's open circuit voltage (OCV) is the measured potential difference when no loads are applied to the battery. Due to the nature of battery kinetics, it can take upwards of an hour, sometimes even a day, after a load is applied to reach a potential equilibrium and thus have a reliable OCV measurement. In the case of this thesis, the battery was rested over a day between measurements for both battery chemistries. OCV testing is conducted in a way to derive the battery's relationship with its state of charge (SOC). The state of charge is used to describe the amount of capacity the battery has left relative to its rated or measured capacity. For example, a battery at 70% SOC with a rated capacity of 10 Ah would be considered to have ~7Ah left in capacity. Testing is carried out by applying a load at its rated amperage with breaks at

set intervals of SOC (typically 5-10%). In some batteries there is a hysteresis in the SOC vs OCV curves when the test is conducted from a fully charged or fully discharged state.^[13] For the purposes of the following discussions, this will be assumed negligible.

2.1.2 Capacity Testing

In order to properly determine the SOC, the capacity of the battery must be determined. The capacity test is carried out by bringing a battery to a fully charged state and allowing it to rest. Then, it is discharged according to its rated capacity until it reaches the minimum, or cutoff, voltage. The capacity is extracted from the test by integrating the current from the beginning to the end of the discharge yielding a value in Ah.

2.1.3 Additional Testing

In addition to the capacity and OCV testing, some dynamic testing is needed to observe the battery's response to varying loads. Depending on the chemistry of the battery, different testing may be available for modeling engineers to extract the model parameters.

Worldwide Harmonized Light Vehicle Testing

For the purposes of this thesis, the dynamic testing used to develop the lead acid battery models will be the worldwide harmonized light vehicle (WLTP) testing. The WLTP testing is currently phasing out the New European Drive Cycle (NEDC) as laboratory testing to determine vehicle energy consumption and emissions within the EU.^[14,15] While the WLTP test is given as a vehicle speed profile, it may be transformed into a power load profile using vehicle simulation software. This vehicle test is considered energy neutral so that the total Ah discharged from the battery are nearly equal to the Ah charged. This means the battery should start and end at the same SOC

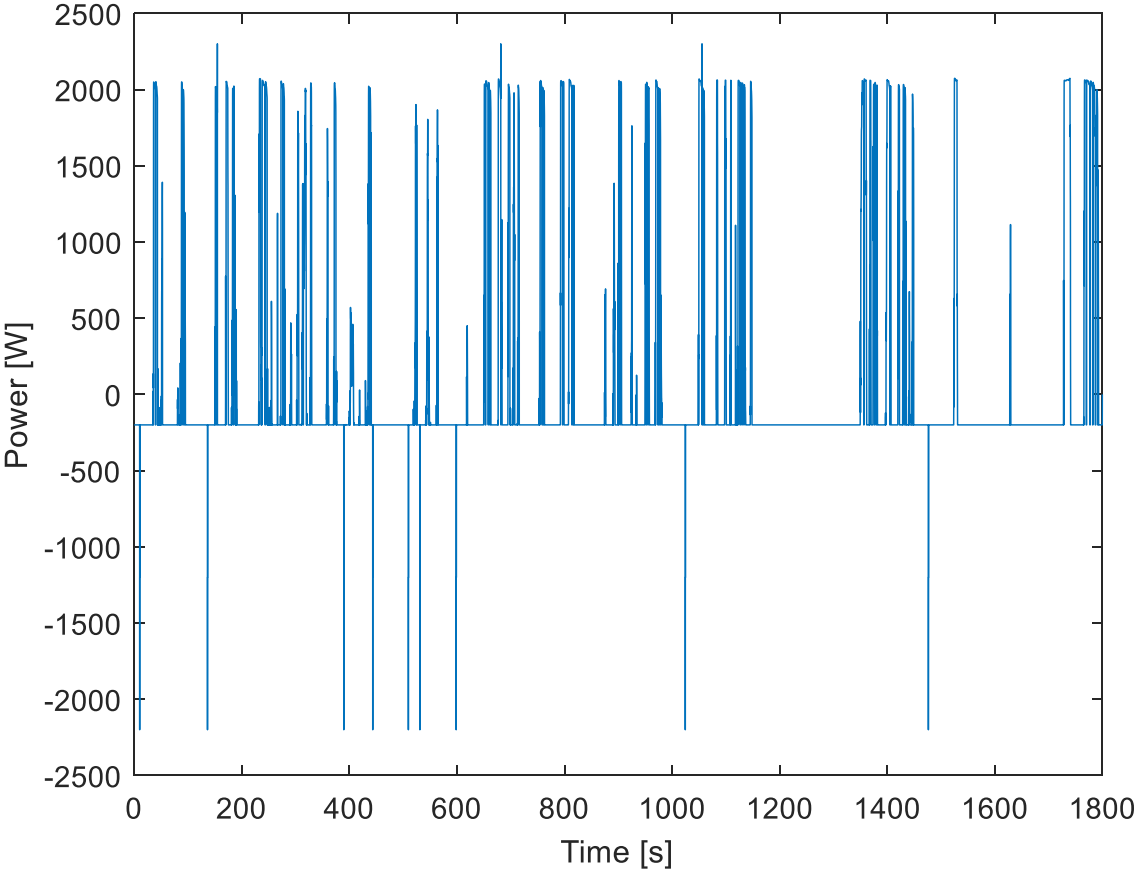


Figure 1: Example of low load power profile for worldwide harmonized light vehicle testing procedure (WLTP)

level. The test is 30 minutes long with loads meant to mimic a real driving profile. An example of the power curve extracted from a vehicle simulation is shown in Figure 1.

Hybrid Pulse Power Characterization Testing

The dynamic testing used to develop lithium ion battery models will be multi current hybrid pulse power characterization (HPPC) testing. HPPC testing is used to understand the dynamic response of a battery at different levels of state of charge. At predetermined intervals (usually meant to line up with 10 % SOC increments) the battery is subjected to separate discharge and charge pulses at a single current for 30 seconds each. The battery is then discharged (or charged) to the following SOC level before it is allowed to rest and the pulse is repeated. In order to create non-ideal test

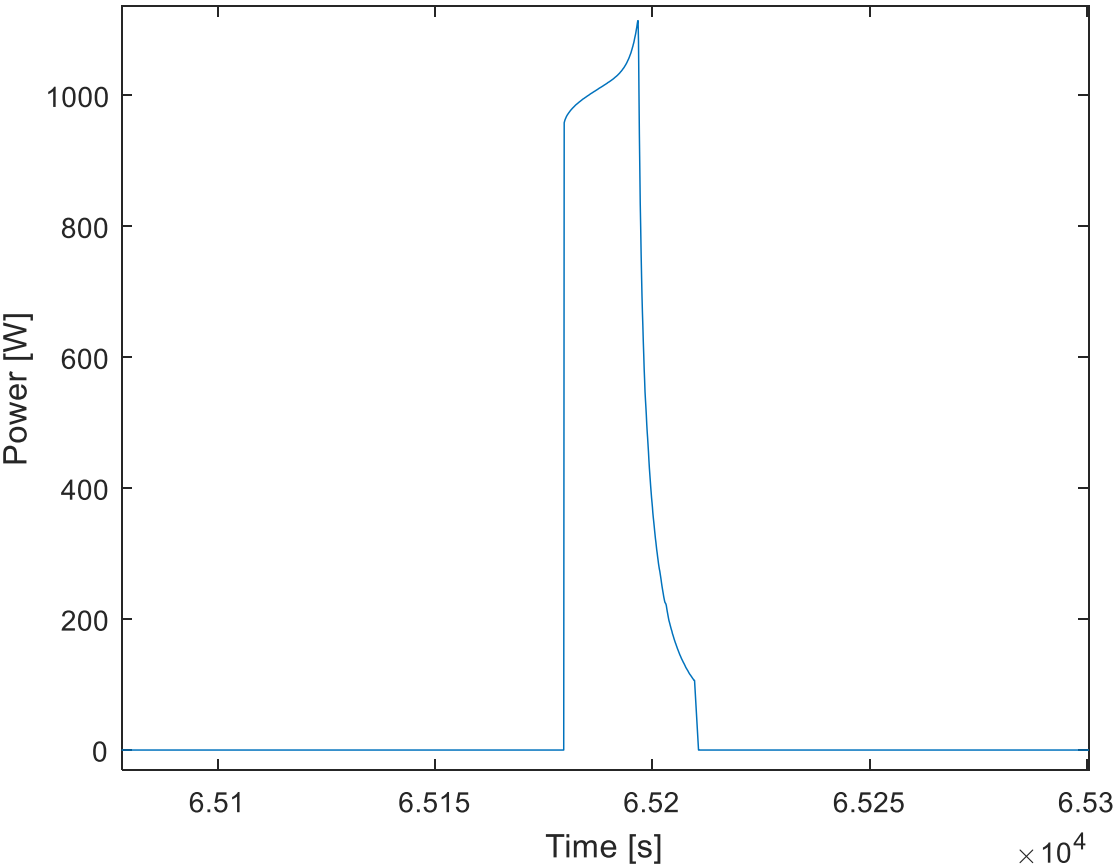


Figure 2: Zoomed in look at high power level HPPC pulse @ 25C for lithium ion cell

data for the purposes of this thesis, the current of charge and discharge was varied from low to high levels. An example of an HPPC charge pulse at a high level of current is given in Figure 2.

2.1.4 Voltage Limits & Testing

When designing the WLTP and HPPC tests for model generation, the intensities of the loads are typically chosen to avoid reaching voltage limits. Voltage limits are imposed to keep a battery from reaching dangerous levels of electric potential. The upper voltage limit is set to keep the battery from thermal runaway and lithium plating in lithium batteries and over gassing in lead acid batteries. The lower voltage, or cutoff voltage, is set to keep the battery from irreversible capacity loss and resistance increase.

Together, they provide a voltage window (Table 1) with which the battery may operate freely while under an applied load.

Table 1: Voltage limits used in testing of lead acid and lithium ion batteries

<i>Battery Chemistry</i>	<i>Upper Limit [V]</i>	<i>Lower Limit [V]</i>
Lead Acid	14.8	6
Lithium Ion	2.8	1.9

When a voltage limit is reached, the battery tester will switch to a constant current, constant voltage charge method for the remaining duration of the load. This means the current is tapered while holding the voltage at the imposed limit – a phenomenon which is not representative of the actual battery behavior. When datasets contain voltage limited pulses, they can impact the accuracy of the battery model derived from them.

It is therefore ideal for tests to be developed to avoid the voltage limits. However, this is not always possible due to time and monetary constraints. Additionally, since batteries are often charged with constant voltage in a vehicle setting, it might also be beneficial to subject the batteries to similar conditions in the test data used for model generation. Assuming a dataset must contain voltage limits, it is desirable to use this data to produce reliable models.

2.2 Battery Modeling

2.2.1 Model Selection

There are three main categories of battery modeling: physical based models, statistical based mathematical models, and equivalent circuit models. Each model subsection has its own pros and cons in both research and industry.

Physical based models are built from first principles with the fewest number of assumptions possible. One of the most popular physical battery models was developed by John Newman and is known as the porous electrode theory (PET).^[17-19] While there are versions of the PET developed for both lead acid batteries and lithium ion batteries, the implementation of these models requires a multitude of characterization tests to determine the appropriate constants, and a significant computing power.

Statistical based mathematical models can also be very useful at predicting trends in battery production or performance.^[20,21] However, these models must be founded on a large enough sample size – which translates into a high up front cost to develop. Like

any statistical model, there might also be an unseen bias if the sample size is not fully understood. These models also tend to be high in mathematical complexity.

The last common battery modeling method is known as equivalent circuit modeling.

These models, though derived from physical assumptions, require less complexity than pure physical models.^[6-10] Therefore, in industry, they are seen as an acceptable middle ground due to their low cost of development and moderate to high accuracy in prediction.

Table 2: Battery model classifications and trade offs

<i>Model Classification</i>	<i>Benefits for Selection</i>	<i>Negatives for Selection</i>
Physical Model	High accuracy, greatest level of understanding	Long run time, large number of parameters
Statistical Based Model	Easy to assess trends, good snapshot of battery behavior	Large sample population required, may have unseen bias
Equivalent Circuit Model	Moderate accuracy, quick development and implementation	Less accurate than physical model, less insight into battery chemistry

2.2.2 Equivalent Circuit Modeling

The equivalent circuit model (ECM) transforms the complexity of a battery's electrochemistry into a simple circuit with a few elements. The goal of the model itself is to take an input usage profile, in either current or power, and predict the battery's voltage and power performance. The idea of an equivalent circuit allows for complex processes in the battery to be distilled into simple elements. While only three ECMs are

outlined and discussed in this thesis, more complex ECMs are capable of offering higher accuracy. However, in an effort to characterize ECM behavior for a new type of testing data, it is important to slowly build in complexity. It is also assumed that the more complex ECMs will follow the trend set in the discussion from these simpler models.

Internal Resistance ECM

A very basic form of equivalent circuit model is generated by connecting an ideal voltage source which represents the OCV to a resistor which represents the internal

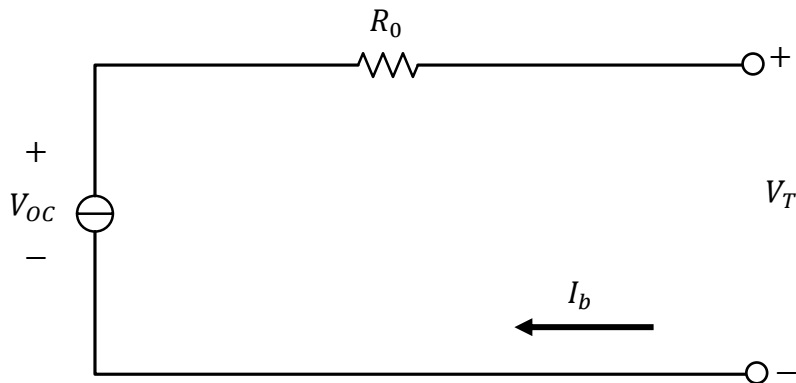


Figure 3: *Internal Resistance Equivalent Circuit Model schematic*

battery resistance. While an even simpler approach might have a fixed OCV, an improvement can be made through the relationship of OCV and SOC. In all subsequent model discussions, it is assumed the OCV is a function of SOC as described by the OCV/SOC testing. The resistance is used to model the instantaneous voltage drop when discharging and similarly the voltage increase when charging the battery. This term therefore is intrinsic to the battery within the context of this model. The schematic for the internal resistance model is shown in Figure 3. with the governing equation (1).

$$V_T = V_{OC} - R_0 I_b \quad (1)$$

Where V_T is the terminal voltage, V_{OC} is the open circuit voltage, R_0 is the internal battery resistance, and I_b is the current flow of the battery.

Thevenin Battery ECM

An improved and slightly more complex equivalent circuit model is referred to as the Thevenin battery model. In this model, there is an additional resistor and capacitor which are in parallel to each other but in series with the previously established voltage source and resistor. The added resistor/capacitor network (RC block) are used to model the dynamic response of the battery. Specifically, these two components are thought to represent the polarization of the battery during a charge or discharge. Together they help to model the voltage relaxation that occurs during and after a charge/discharge. Their product is also commonly referred to as the time constant, τ_1 . The adjusted diagram is shown in Figure 4 along with governing equations (2) & (3).

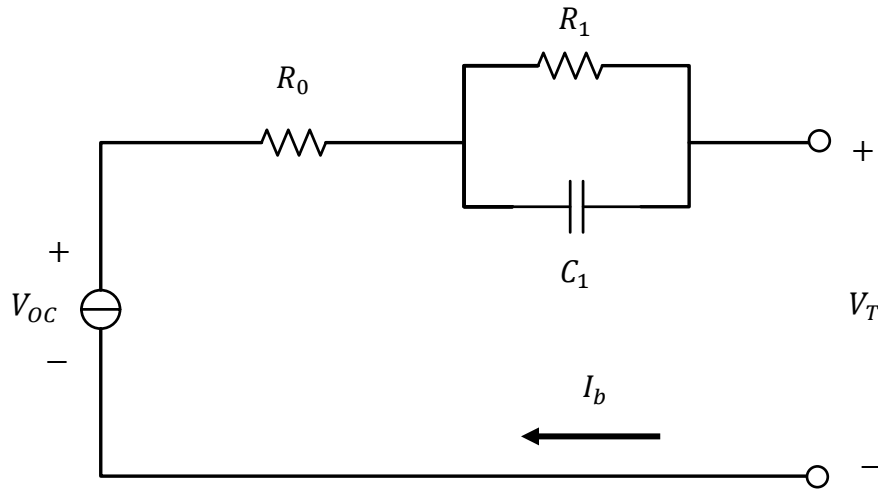


Figure 4: Thevenin Equivalent Circuit Model schematic

$$V_T = V_{OC} - I_b R_0 - v_1 \quad (2)$$

$$\frac{dv_1}{dt} = -\frac{v_1}{R_1 C_1} - \frac{I_b}{C_1} \quad (3)$$

Where R_1 and C_1 are the added resistor/capacitor to describe the dynamic battery behavior under a load, v_1 is the voltage across the RC circuit, and $\frac{dv_1}{dt}$ is the time differential of the voltage across the RC circuit which will be discretized and solved at each time step.

Modified Thevenin Battery ECM

One final model will be considered. This model will be referred to as the modified Thevenin ECM. Similar to the Thevenin model described previously, this model has a voltage source, resistor, and parallel branch of resistor/capacitor. The modification is made by allowing for two time constants; one for charging and one for discharging. With this modification, the model is less inhibited when there is an imbalance in charging and discharging constant voltage regions as is often the case.

2.2.3 Discretization of Model Equations

In order to solve these models, they are all discretized. The schemes for each discretization method are described in detail below.

IR Model

Since there are no time derivatives involved outside of SOC tracking within this model, the resulting equations (4) & (5) are very simple.

$$V_T(t) = V_{OC}(SOC(t)) - R_0 I_b(t) \quad (4)$$

$$SOC(t) = SOC(t - \Delta t) + I_b(t) * \frac{\Delta t}{Q} \quad (5)$$

Where Q is the battery capacity, Δt is the sampling rate, and $V_{OC}(SOC(t))$ is solved using a linear 1D interpolation lookup table generated during OCV testing.

The SOC is tracked through basic current integration, also known as coulomb counting.

Thevenin & Modified Thevenin Models

Beginning with equations (2) & (3), the system is solved accordingly

$$V_T(t) = V_{OC}(SOC(t)) - R_0 I_b(t) - v_1(t) \quad (6)$$

Where $SOC(t)$ and subsequently, $V_{OC}(SOC(t))$ are solved in the same way as the IR model.

Additionally, since equation (3) is of the form

$$\frac{dx}{dt} + ax(t) = -bu(t) \quad (7)$$

Where

$$a = \frac{1}{R_1 C_1} \quad (8)$$

$$b = \frac{1}{C_1} \quad (9)$$

$$x(t) = v_1(t) \quad (10)$$

$$u(t) = I_b(t) \quad (11)$$

Then the equation is of the state space configuration and the discretized time domain solution is

$$v_1(t) = v_1(t - \Delta t) * \exp\left(-\frac{\Delta t}{R_1 C_1}\right) - R_1 I_b(t) * \left(1 - \exp\left(-\frac{\Delta t}{R_1 C_1}\right)\right) \quad (12)$$

In the case of the modified Thevenin model, the time constant parameters will be adjusted according to the following logic in equation (13).

$$R_1 C_1 = \begin{cases} \text{Discharging,} & I_b(t) < 0 \\ \text{Charging,} & I_b(t) \geq 0 \end{cases} \quad (13)$$

2.2.4 Initial Guess Determination for Model Parameters

Finally, the model coefficients are fit using the MATLAB function `nlinfit` with initial guesses of the coefficients based on simple extraction from a sample pulse in the dataset.

Initial Guess R_0

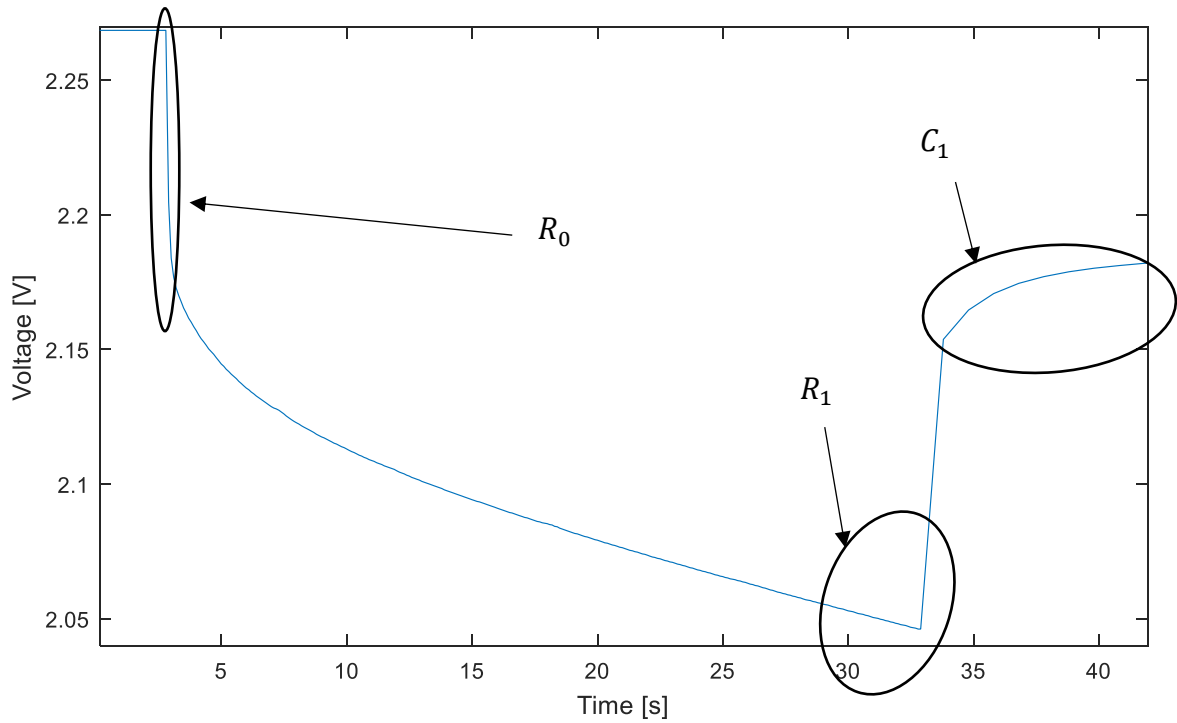


Figure 5: Initial guess parameter extraction. R_0 taken from initial 10 ms of pulse, R_1 taken from final voltage of pulse, C_1 taken from relaxation after the pulse

Since the R_0 parameter represents the internal resistance, an initial guess can be taken from any pulse within the dataset. The internal resistance should be represented by the voltage drop of the battery at the instantaneous application of a load. Therefore, by taking a pulse like that shown below, R_0 may be estimated according to equation (14).

$$R_0 = \frac{\Delta V}{\Delta I} \text{ (for initial 10 ms)} \quad (14)$$

Initial Guess R1, C1

Both R1 and C1 together represent the time constant of the model, or the polarization of the battery. The initial guess may be determined from the same pulse. R1 may be calculated directly from equation (15). From previous work it is understood that the time constant for lead acid and lithium ion batteries should be on the order of 10-30 seconds. Thus, C_1 may be estimated from R_1 according to equation (16). Since these serve as initial guesses, accuracy is of little importance.

$$R_1 = \frac{\Delta V}{\Delta I} - R_0 \text{ (for duration of entire pulse)} \quad (15)$$

$$C_1 = \frac{\tau_1}{R_1} \quad (16)$$

If there is no previous knowledge at hand for a time constant estimation, C1 may be taken from the total relaxation time after the pulse is completed assuming there is sufficient time without an additional load.

2.3 Model Verification

The final step in battery model generation is being able to verify that the model is accurate. As noted in the derivation of section 2.2, each equivalent circuit model has an input current I_b and an output terminal voltage V_T which are both measured during testing. Therefore, when characterizing the accuracy of each ECM, the voltage responses will be the primary focus. Outside of visual inspection, three statistical approaches will be taken into account to define the accuracy of each model: the maximum error in voltage, mean absolute error in voltage, and the root mean squared error (RMSE) of the voltage for the duration of the profile in question. The combination of these three metrics provides the range of error as well as the precision of the model.

Additionally, when characterizing methods which improve accuracy for ECMs in vehicle applications, the power, state of charge, current, voltage, and energy throughput will be considered. Since the battery models predict voltage from an input current, some modifications will be required towards the implementation of the model. The scheme by which a power profile will instead be used in order to predict current, voltage, power, and SOC is described in Figure 6.

Once again, in addition to visual inspection, the model's accuracy will be defined by the max, mean and RMS error of each variable. This will allow for a better understanding into whether these models are sufficient to be used in real applications despite the imperfect datasets used to build them.

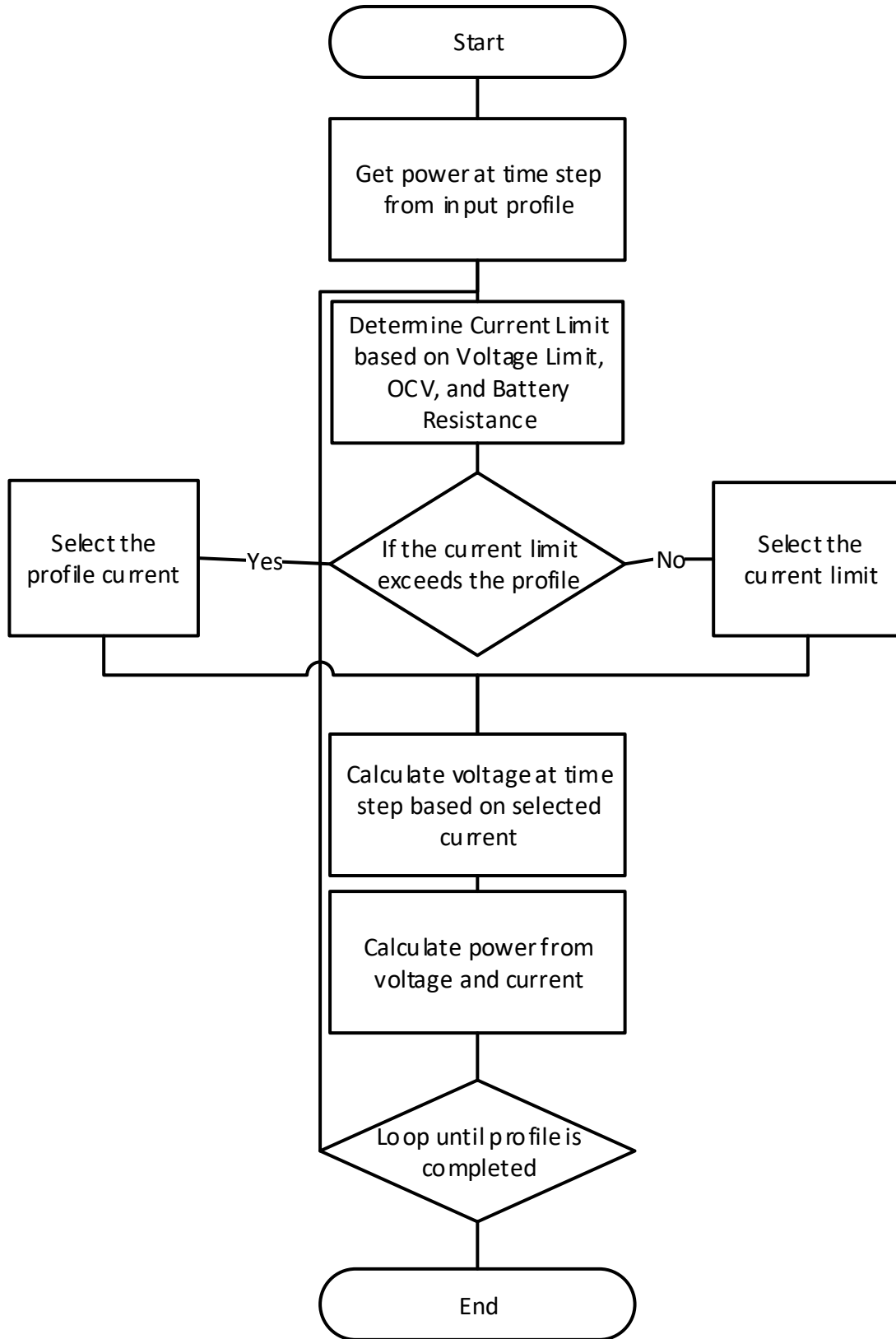


Figure 6: Representation of model implementation to predict performance given an input power profile

3. Generation and Comparison of Equivalent Circuit Models

Three equivalent circuit models (IR, Thevenin, and Modified Thevenin) were considered for modeling the battery's behavior. While it is already understood that an IR model will be less accurate than the other two possible models on ideal datasets, it is important to verify this is still the case when using non-ideal datasets. Since ECMs are well studied in lithium ion battery modeling with ideal datasets, the first focus will be on the HPPC testing of lithium ion batteries. The same methodology will be applied to the WLTP testing of lead acid batteries to verify the consistency between both chemistries.

3.1 Lithium Ion Modeling

HPPC testing was carried out at four levels of current per charge/discharge at each SOC level from 90% to 10%. A total of 6 Lithium Ion cells were tested at 25 degrees Celsius. To observe the impact of voltage limited regions on model accuracy, the charge and discharge pulses at 80% from HPPC tests were pieced together in order of increasing current level. Data was captured at a rate of 10 ms. A summary of the current level of each pulse is given in Table 3.

Table 3: Multi-current description for charge and discharge at 80% SOC in HPPC testing

<i>Current Level</i>	<i>Charge [A]</i>	<i>Discharge [A]</i>
<i>Low</i>	120	-200
<i>Moderate Low</i>	250	-260
<i>Moderate High</i>	350	-330
<i>High</i>	400	-400

The battery SOC vs. OCV relationship was determined through standard testing and an example of the curve is shown in Figure 7.

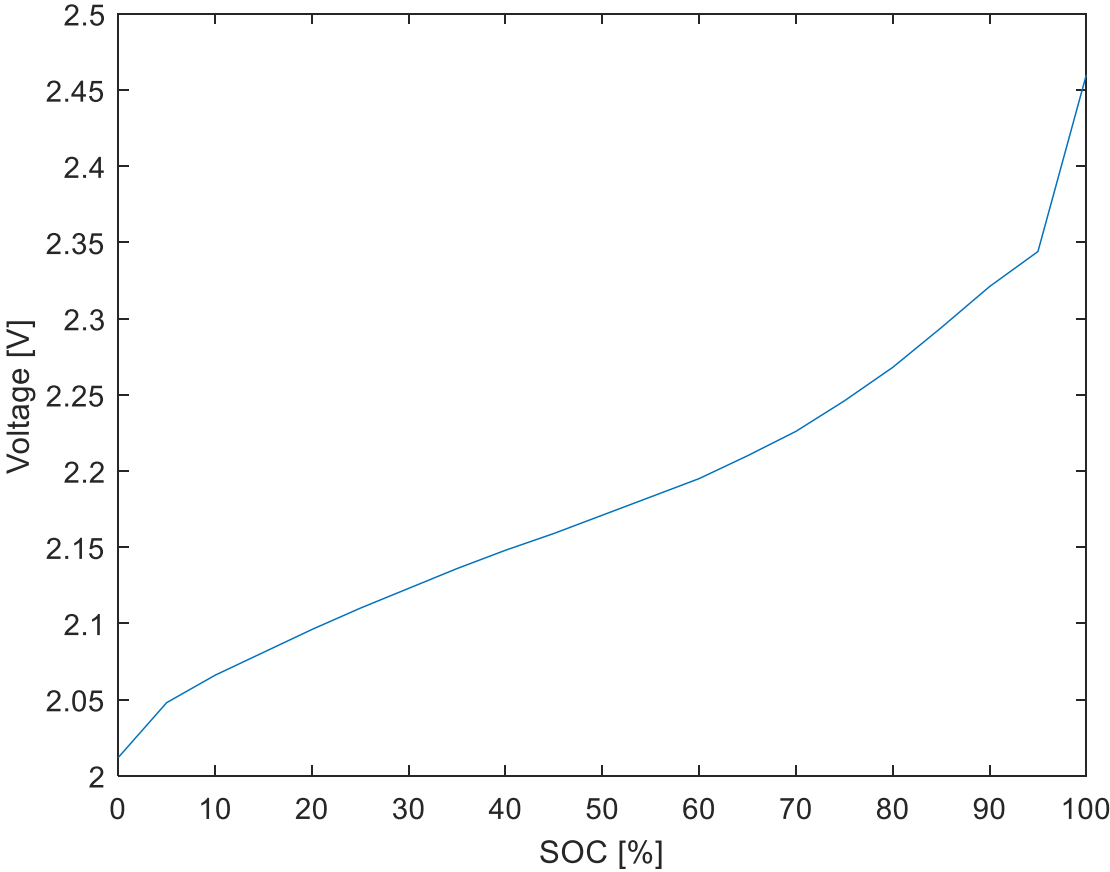


Figure 7: SOC vs. OCV relationship for lithium ion battery used in HPPC testing

The capacity was determined at the start of the test for each cell. An average of the 6 cells was used as the capacity for fitting since the variability among cells was <1%.

3.1.1 Internal Resistance Model

The internal resistance model was fit to the set of HPPC data for each of the 6 cells using an initial guess of 0.0005 Ohm. The R_0 parameter was fit using MATLAB's `nlinfit`. The voltage response is modeled in Figure 8. for the first of the 6 cells using the average R_0 fit. By looking closely at a discharge and charge pulse separately in Figure 9, it is clear that this approach is not complete enough to model the total battery behavior. Though, it models discharge pulses more accurately than charge pulses, likely due to a lack voltage limits.

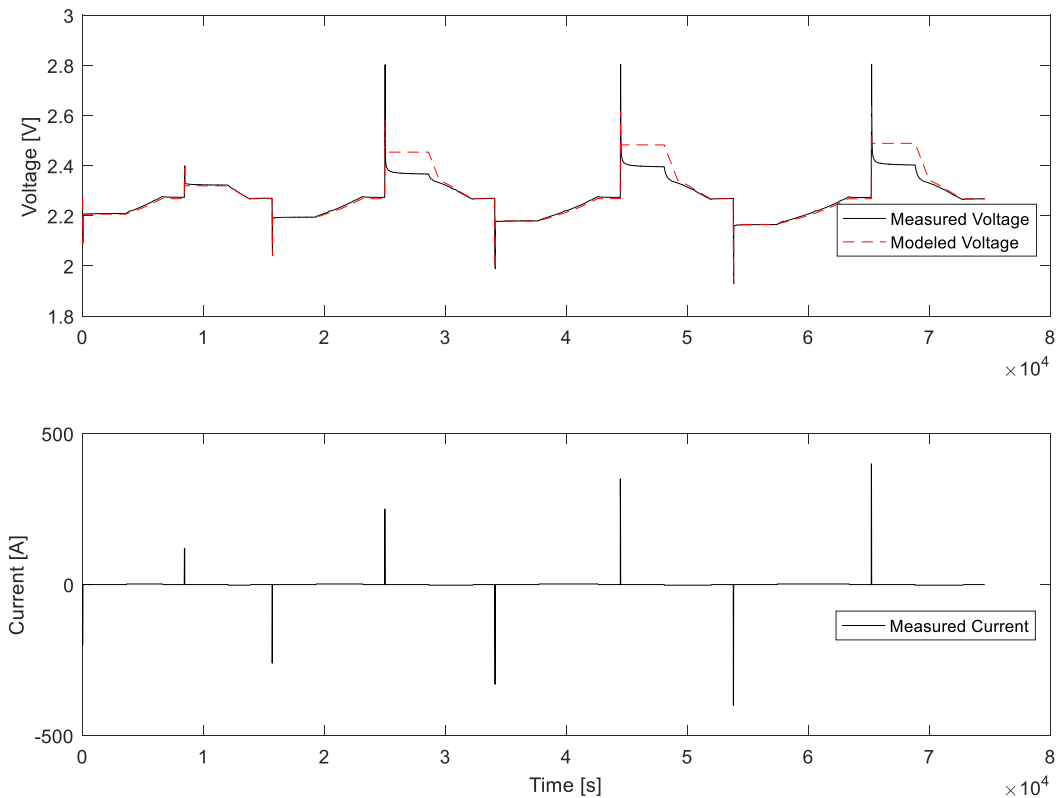


Figure 8: (a) Internal Resistance model comparison of predicted voltage vs. measured test voltage, (b) Measured test current

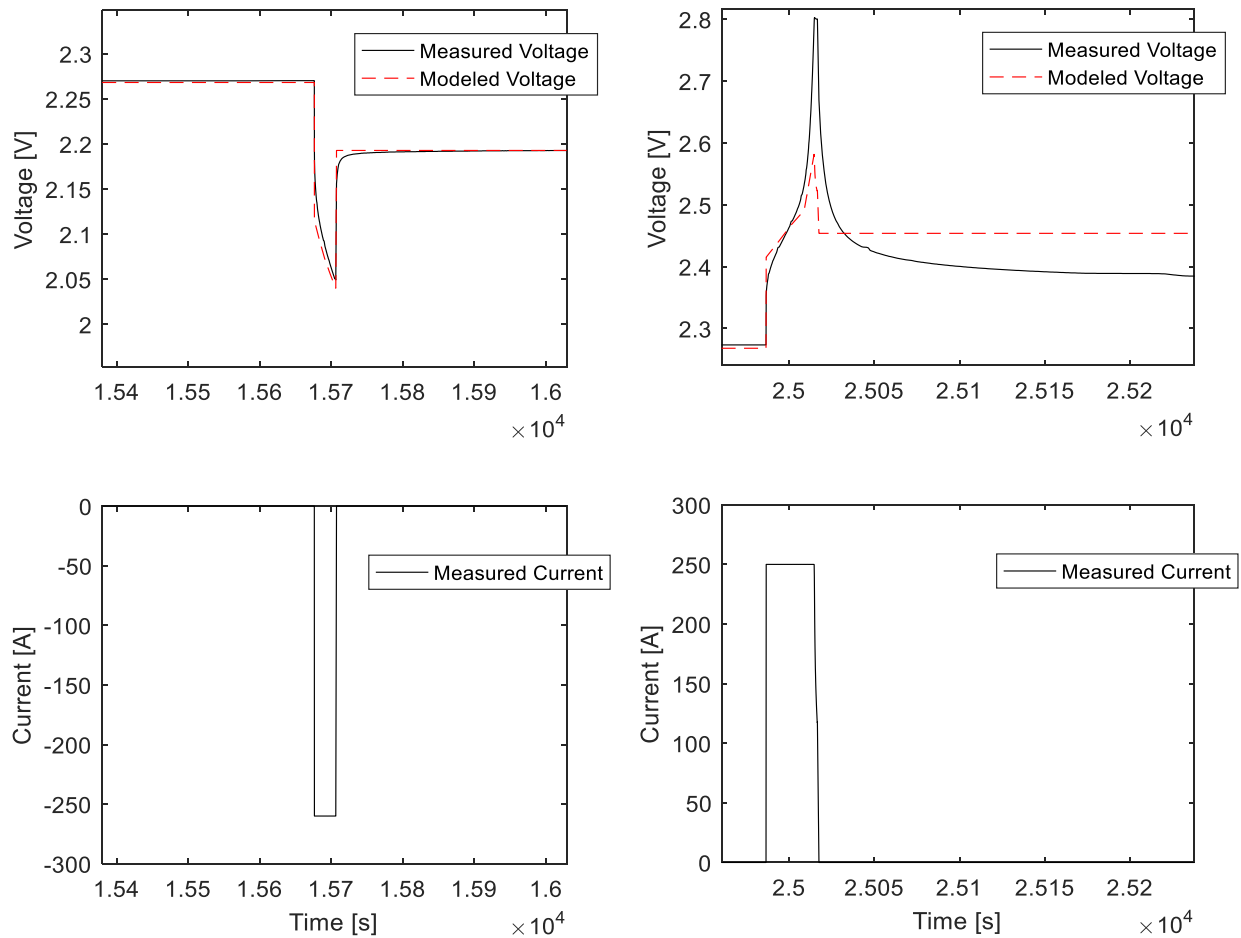


Figure 9: Internal resistance model behavior for lithium ion HPPC testing (a) Predicted vs. measured voltage in moderate low current discharge pulse, (b) Measured current for pulse in (a), (c) Predicted vs. measured voltage in moderate low current charge pulse, (d) Measured current in (c)

Table 4: Summary of accuracy for the internal resistance ECM prediction of lithium ion voltage in HPPC testing

Max error [V]	Mean error [V]	RMS error [V]
0.298	0.025	0.067

A close inspection shows that the voltage appears to be changing non-linearly, which is unexpected in the usage of an internal resistance only ECM. However, due to the high starting SOC, during charge pulses the final SOC is near 100%. By comparing the

curvature with the OCV curve (Figure 7.) in the same range, this non-linearity is accounted for.

3.1.2 Thevenin Battery Model

The Thevenin battery model was fit using `nlinfit` and an initial guess of 0.0005 Ohm for R_0 and R_1 as well as 1000 F for C_1 . An increase in charging voltage accuracy can be

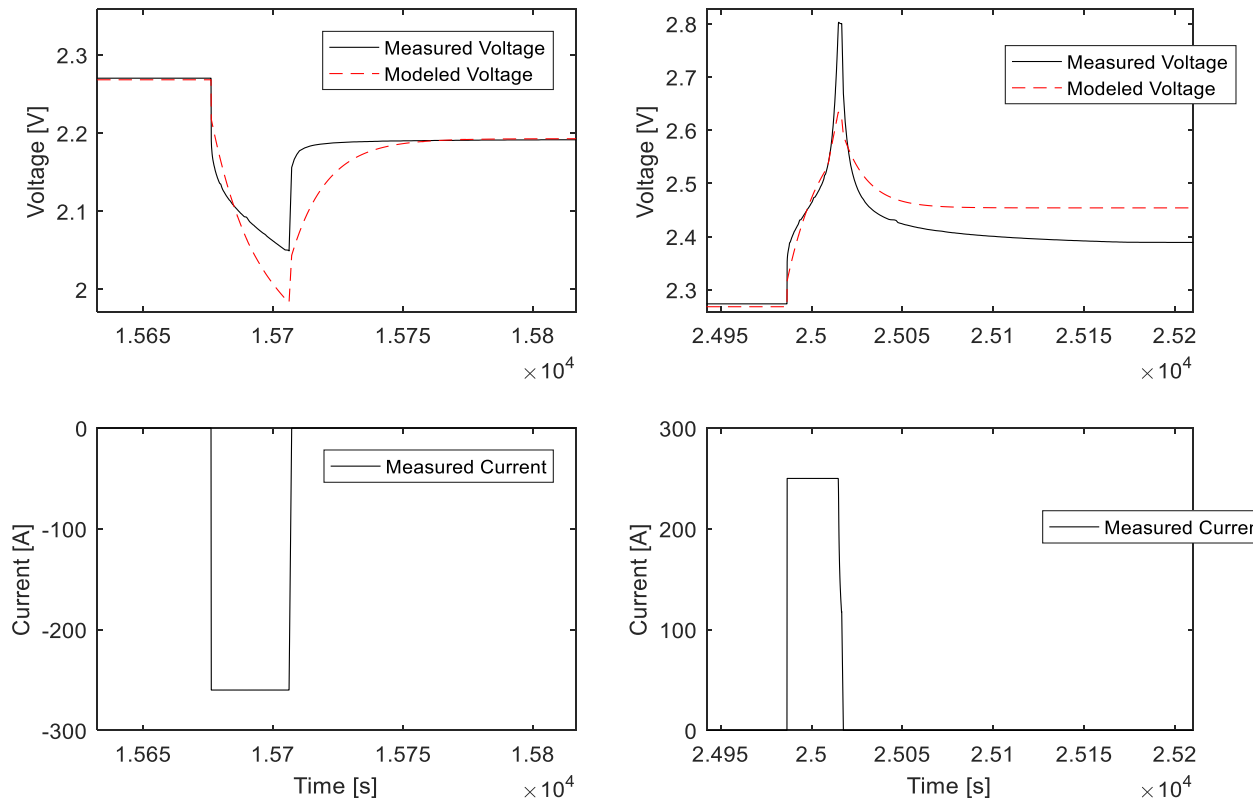


Figure 10: Thevenin model behavior for lithium ion HPPC testing (a) Predicted vs. measured voltage in moderate low current discharge pulse, (b) Measured current for pulse in (a), (c) Predicted vs. measured voltage in moderate low current charge pulse, (d) Measured current in (c)

observed in Figure 10. With this comes a decrease in accuracy in the discharge pulse accuracy. The model does improve overall accuracy by reducing the maximum error by ~0.1 V, but the average error actually increases from 0.025 V to 0.028 V while the RMS error is improved slightly by 0.02 V. The discharge relaxation error can be explained as a result of the voltage limited charging. Since the model only has one time constant,

which is attempting to fit regions in which the voltage is not allowed to relax at a normal rate, the discharge relaxation is equally impacted. This phenomenon should be improved with the modified Thevenin model.

Table 5: Summary of accuracy for the Thevenin ECM prediction of lithium ion voltage in HPPC testing

Max error [V]	Mean error [V]	RMS error [V]
0.201	0.025	0.048

3.1.3 Modified Thevenin Battery Model

Finally, the modified Thevenin model was fit using `nlinfit` in MATLAB with initial guesses of 0.0005 Ohm for R_0 as well as both sets of R_1 , and 1000 for both sets of C_1 . The resulting fit is summarized in the following Figure. 11 & Figure 12. Of the three models

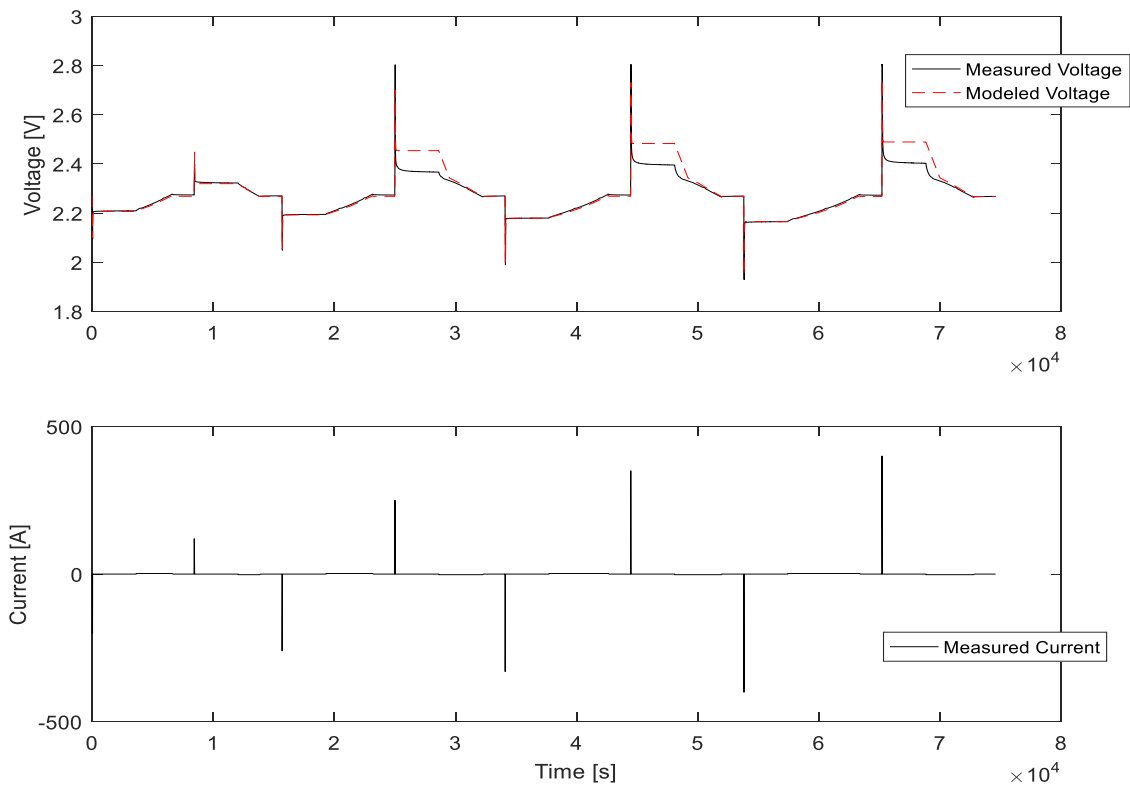


Figure 11: (a) Modified Thevenin model comparison of predicted voltage vs. measured test voltage, (b) Measured test current

considered, it has the lowest maximum error and RMS error with little change in mean error. As predicted, by unlinking the charge and discharge time constants, the voltage

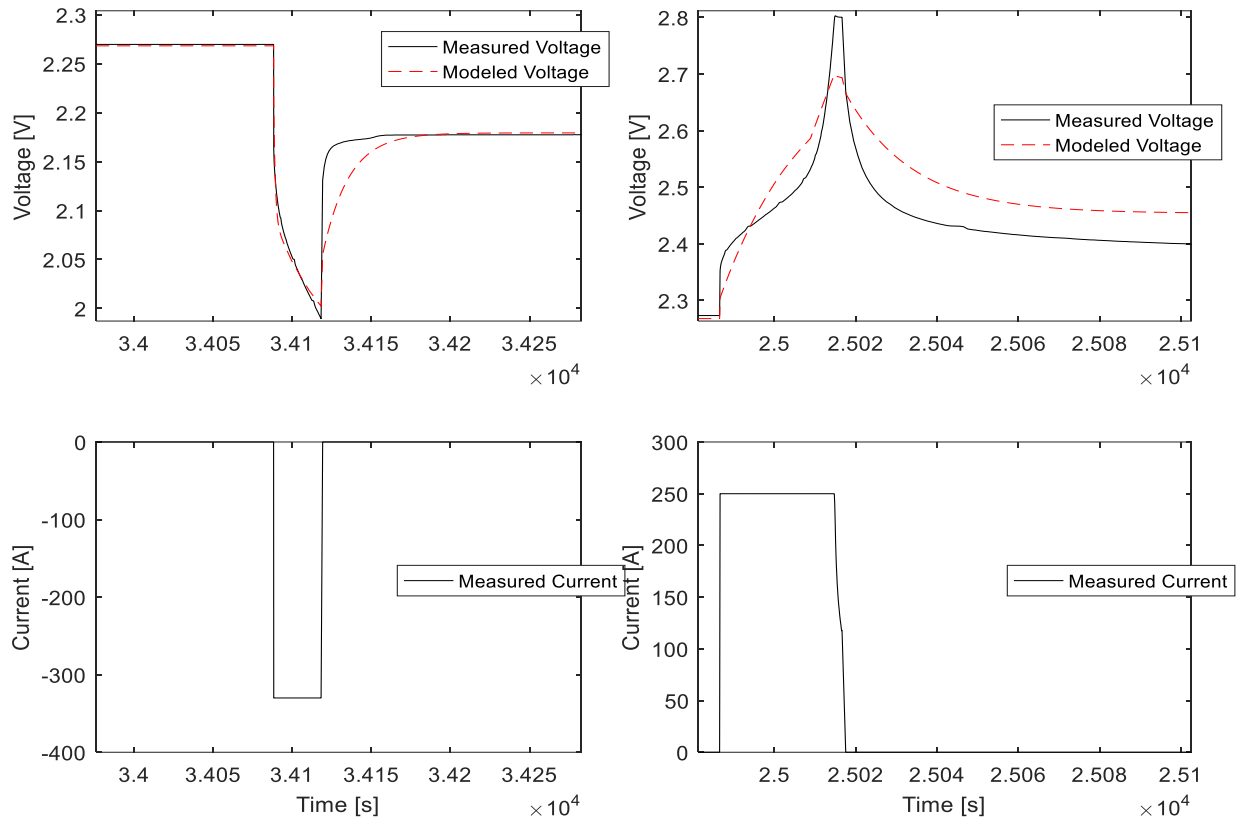


Figure 12: Modified Thevenin model behavior for lithium ion HPPC testing (a) Predicted vs. measured voltage in moderate high current discharge pulse, (b) Measured current for pulse in (a), (c) Predicted vs. measured voltage in moderate high current charge pulse, (d) Measured current in (c)

limiting behavior no longer impacts the discharge relaxation.

Table 6: Summary of accuracy for the Modified Thevenin ECM prediction of lithium ion voltage in HPPC testing

Max error [V]	Mean error [V]	RMS error [V]
0.140	0.028	0.032

While the mean error in voltage is a few mV higher than the other two models, both max error and RMS error are approximately 30% lower. Therefore, the model may still be

considered the best of the three. It should also be noted that Figure 12. shows the response on the moderate high current pulses to emphasize the improved accuracy of the model despite the increased load.

3.1.4 Lithium Ion Fitting Summary

It was expected that the increased complexity of the ECMs would result in a more accurate fit. This was shown to be the case as the most complex, the modified Thevenin model, was also the most accurate with the lowest maximum voltage error and the lowest voltage RMS error. A full summary of the accuracy for each model is given in Table 7.

Table 7: Summary of accuracy for each model considered in lithium ion HPPC testing

<i>Model</i>	<i>Max error [V]</i>	<i>Mean error [V]</i>	<i>RMS error [V]</i>
IR	0.298	0.025	0.067
Thevenin	0.201	0.025	0.048
Modified Thevenin	0.140	0.028	0.032

Despite the improvements made by each model, it is clear that limiting the voltage of charge pulses in the moderate high and high current ranges limit the accuracy of the fit. This can be shown in greater detail by using only the lowest current pulses (charge and discharge) to generate a basic Thevenin model. The results of which are shown in Figure 13.

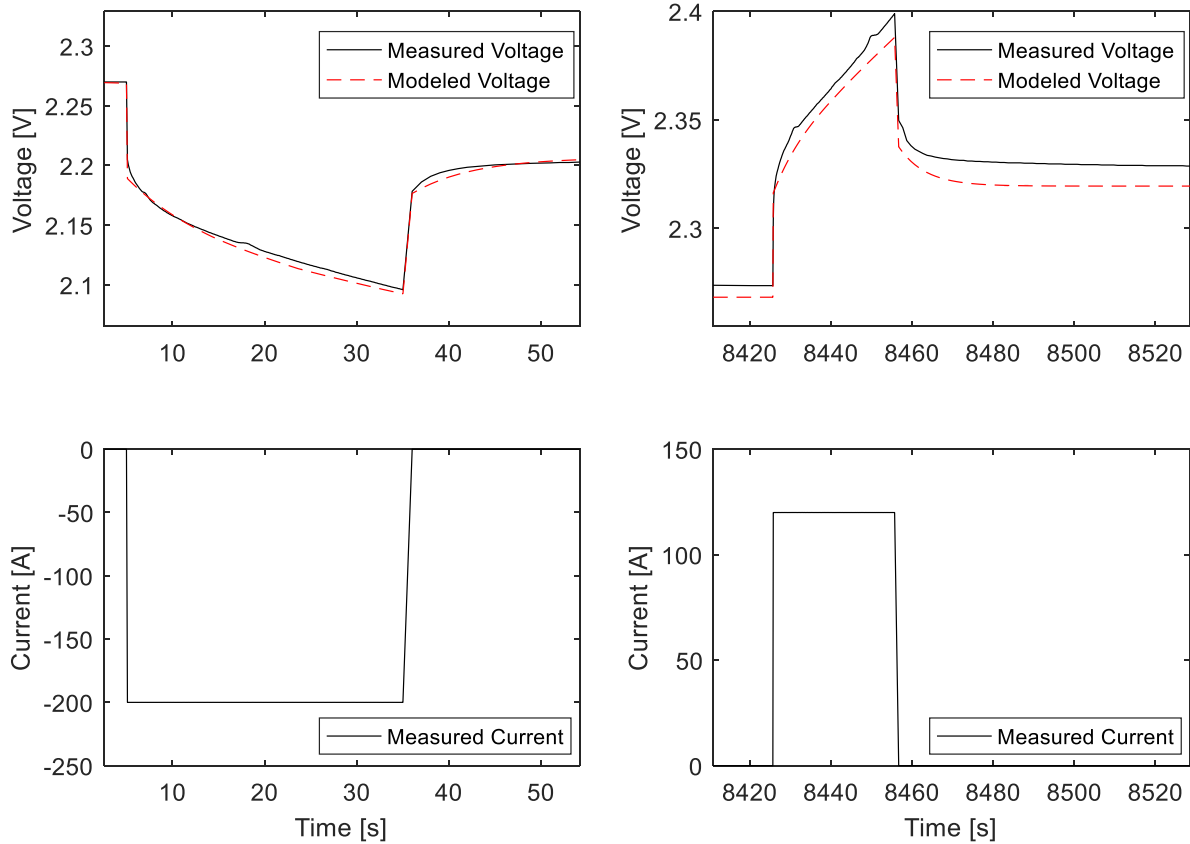


Figure 13: Thevenin model behavior for lithium ion HPPC testing when fitting for only the low current pulses (a) Predicted vs. measured voltage in low current discharge pulse, (b) Measured current for pulse in (a), (c) Predicted vs. measured voltage in low current charge pulse, (d) Measured current in (c)

It is also worth noting that in the case of an HPPC test, it is typically easy to avoid hitting voltage limits by reducing the current used in testing the moderate high, and high pulses. There is a tradeoff in limiting the model's performance in high current regions that stems from this.

It will be the goal of the final section of this thesis to provide a way for the modeling engineer to adapt the set of data with voltage limits so that the accuracy more closely represents that of Figure 13.

3.2 Lead Acid Modeling

Since the impact of voltage limits were aptly described for lithium ion cells, it is the goal of this section to show a similar trend across each model so that voltage limiting impact may be assessed independently of battery chemistry.

The WLTP test was used to capture both voltage and current response of 3 separate lead acid batteries of the same size and build. The WLTP cycling was repeated 5 times on each battery under a scaled load to mimic real vehicle loads. Data was captured at 10 ms intervals for the duration of the cycling and carried out at 25 degrees Celsius.

The initial SOC for each WLTP cycle was 80%. This was achieved by using a regeneration sequence after each WLTP cycle to account for any imbalance in charged and discharged Ah over the cycle. Batteries were then allowed to rest prior to repeating the WLTP cycle so that the OCV may be measured to confirm the SOC level. Since the WLTP testing is meant to be energy neutral, the regen sequence was of short duration.

The battery SOC vs. OCV relationship was determined separately. An example of the nonlinear relationship is shown in Figure 14.

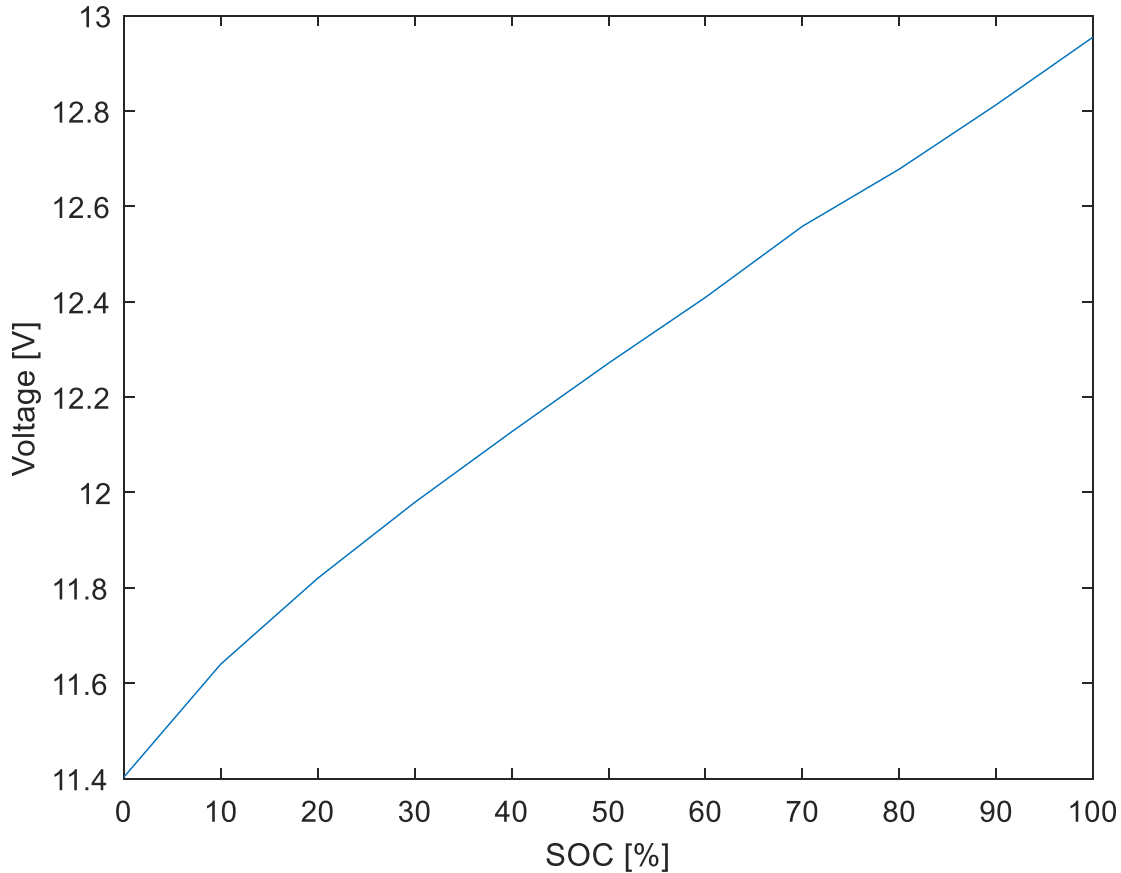


Figure 14: SOC vs. OCV relationship for lead acid battery used in WLTP testing

The capacity was determined for each of the three lead acid batteries. An average value was used for the model fitting procedure as the variability was low enough to be negligible (<1%).

For each model, the coefficients were determined at each individual cycle and then averaged together across all 15 cycles. The accuracy of the model was determined by using the average coefficients to model each of the 15 profiles. Visual inspection as well as max voltage error, mean voltage error, and RMS voltage error were all calculated for the total of the 15 cycles using the single set of model coefficients.

3.2.1 Internal Resistance Model

The first and simplest model considered was the internal resistance model. Due to the simplicity of this model, only one coefficient was determined. For consistency, the value of R_0 was determined using the MATLAB function `nlinfit` with an initial guess of 0.01 Ohm for R_0 . The resulting voltage curve is shown for one representative cycle of WLTP below. As expected, the transient behavior is not well modeled. Nonetheless, it is still capable of providing a good estimation of the battery's voltage response during charge, however it produces a maximum error of $\sim 2V$ which is quite high.

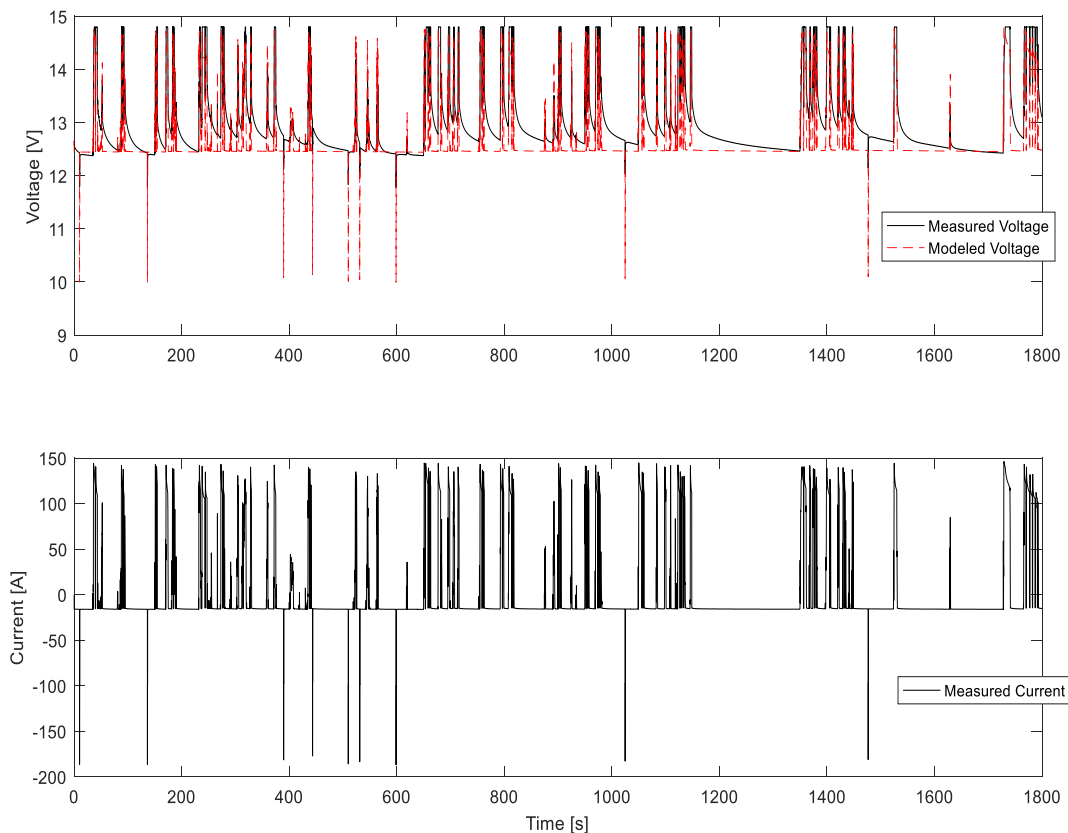


Figure 15: (a) Internal Resistance model comparison of predicted voltage vs. measured test voltage, (b) Measured test current

Table 8: Summary of accuracy for the Internal Resistance ECM prediction of lead acid voltage in WLTP testing

Max error [V]	Mean error [V]	RMS error [V]
2.18	0.24	0.34

Relative to the overall range in battery voltage (6-14.8 V), the maximum error translates to ~25% relative error which when compared to the scaled relative maximum voltage error in lithium ion IR modeling (~33%) shows there is a consistent level in error.

3.2.2 Thevenin Battery Model

The second model considered was the Thevenin battery model which includes an additional parallel resistor/capacitor branch in order to model the transient behavior.

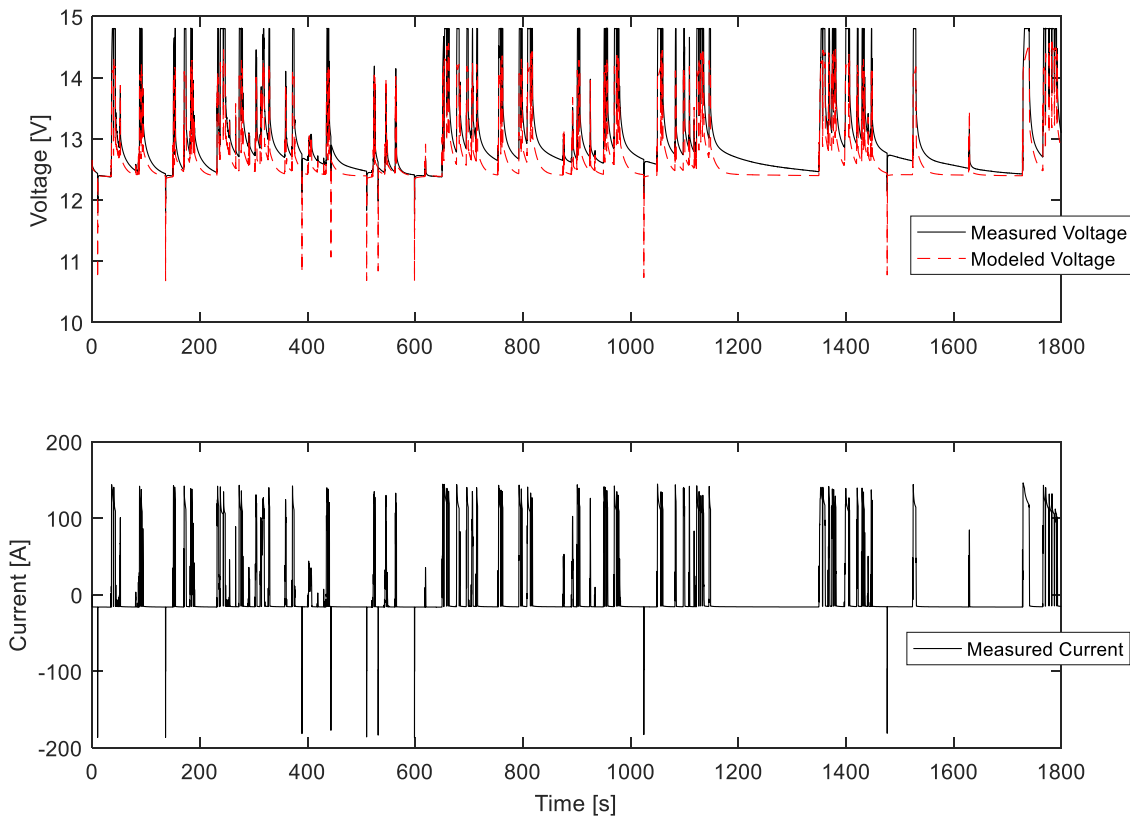


Figure 16: (a) Thevenin model comparison of predicted voltage vs. measured test voltage, (b) Measured test current

Though the value of R_0 in theory should not change from the previous fit, it was refit

along with R1 and C1 for consistency. The values were fit using nlinfit in MATLAB with initial guesses of 0.01, 0.008, and 1250 for R0, R1, and C1 respectively. The resulting voltage response on a representative WLTP cycle is shown below. It appears that while the transient behavior is more aptly captured, the inclusion of voltage limits in the fitting data set alters the accuracy of the fit as expected. Additionally, the maximum voltage error is still ~1.36 V (15%). The improvements of the lead acid Thevenin model in relative maximum error closely match those of lithium ion with 10% and 11% improvements respectively. There was minimal improvements in RMS and mean error however.

Table 9: Summary of accuracy for the Thevenin ECM prediction of lead acid voltage in WLTP testing

<i>Max error [V]</i>	<i>Mean error [V]</i>	<i>RMS error [V]</i>
1.36	0.23	0.29

3.2.3 Modified Thevenin Battery Model

The last model is expected to be the more accurate of the three considered as was shown for lithium ion. The initial guesses were the same as those used for the Thevenin model. Additionally, the values of R1 and C1 were kept the same for both charge and discharge. The model was solved using nlinfit in MATLAB. The resulting fit is clearly the best of the three models considered as the relaxation is well matched. However, there are still signs of the voltage limit behavior impacting the R0 fitting.

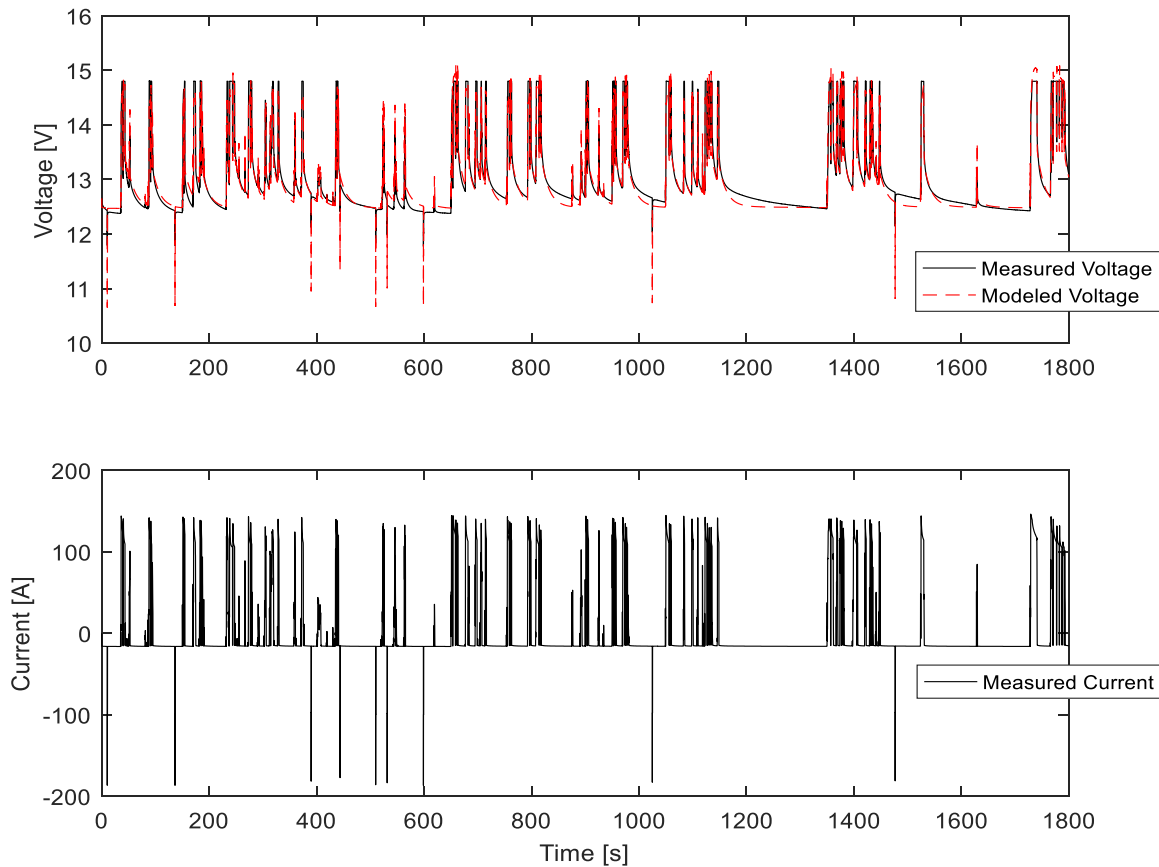


Figure 17: Modified Thevenin model comparison of predicted voltage vs. measured test voltage, (b) Measured test current

Table 10: Summary of accuracy for the Modified Thevenin ECM prediction of lead acid voltage in WLTP testing

<i>Max error [V]</i>	<i>Mean error [V]</i>	<i>RMS error [V]</i>
1.30	0.16	0.25

As was the case with the modified Thevenin model in lithium ion cells, the RMS and maximum error are both improved. In this case, the mean error is also improved from 0.23 to 0.16 V. The final relative maximum error of both chemistries is ~15%.

3.2.4 Lead Acid Fitting Summary

As expected, there is once again a noticeable improvement in battery voltage prediction from the IR model to the modified Thevenin model. One area of concern may be the over prediction of discharge voltage; however, this is considered an artifact of the ECMs rather than any impact from voltage limits and is thus outside the scope of the thesis.

Table 11: Summary of accuracy for each model considered in lead acid WLTP testing

<i>Model</i>	<i>Max error [V]</i>	<i>Mean error [V]</i>	<i>RMS error [V]</i>
IR	0.298	0.025	0.067
Thevenin	0.201	0.025	0.048
Modified Thevenin	0.140	0.028	0.032

Unlike the lithium ion cells, the relative maximum error was lower initially, however both chemistries saw similar improvements over the range of models considered. Due to the final accuracy of each model (Table 11) it can be taken that the voltage limited behavior impact is in fact independent of the battery chemistry.

3.3 Conclusion

Lead acid batteries follow the same trend as lithium ion batteries with ECM accuracy. The modified Thevenin model produces the highest accuracy fit because it establishes a separate time constant for charge and discharge. However, the charging prediction still has larger error fluctuations due to the voltage limited behavior.

While a moderately accurate fit may be achieved using the modified Thevenin model, even when the dataset contains constant voltage charging regions, it is desirable to

determine a way in which the data may be modified or treated so that the voltage limits have less impact on the resulting fit.

4. Voltage Limit Impact on Fitting Method

So far it is clear that regardless of model selection, the impact of voltage limits in testing is not negligible. However, it is the purpose of this section to determine the best way to obtain the highest value from these datasets without having to rerun testing. Three methods were characterized with the ultimate goal of finding the method that results in the least error.

As was shown in section three, both lithium ion and lead acid batteries are affected in similar ways by constant voltage charging regions. Therefore, since WLTP testing more closely mimics vehicle behavior, it will be used as the dataset for comparison in this section (with lead acid batteries). It is assumed the same methodology would apply to lithium ion batteries as well.

Of the 15 cycles used for model validation, cycle three was used as the representative cycle in visual inspection since it was the intermediate cycle of the test profile for the first battery. The behavior across each of the three batteries was similar enough that only one battery cycle will be used for visual inspection. However, all 15 cycles were used for statistical analysis.

Each method was compared in their ability to accurately predict and model the power, SOC, voltage, current, and energy throughput of a WLTP test profile conducted at a different load level than that used to build the model.

Due to the high level of accuracy from the modified Thevenin model and to simplify the discussion, it will be the only ECM considered.

4.1 Baseline Case – No Modification

The first method considered is to fit the data without any adjustment as was discussed in the previous section. The fitting performance can be observed in both Figure 18. and Figure 19. Since the validation profile in use is the higher load WLTP profile, more voltage limiting regions are experienced across each of the 15 cycles.

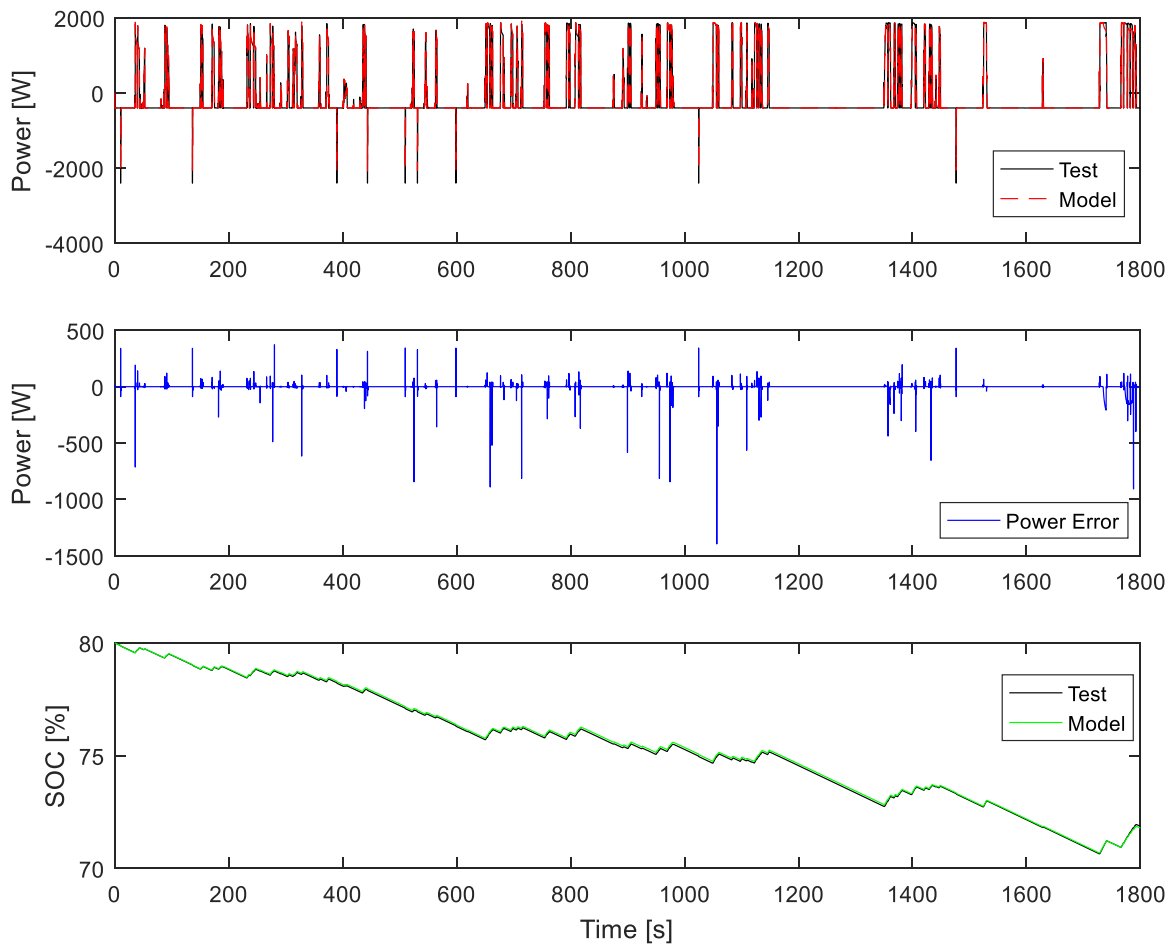


Figure 18: Baseline case fitting method for Modified Thevenin ECM of high load WLTP power profile (a) Measured vs. predicted power, (b) Instantaneous, absolute error in power, (c) SOC calculated from test vs. modeled SOC

Using the same statistical metrics as section 3, the accuracy of the model in predicting key metrics is summarized in Table 12.

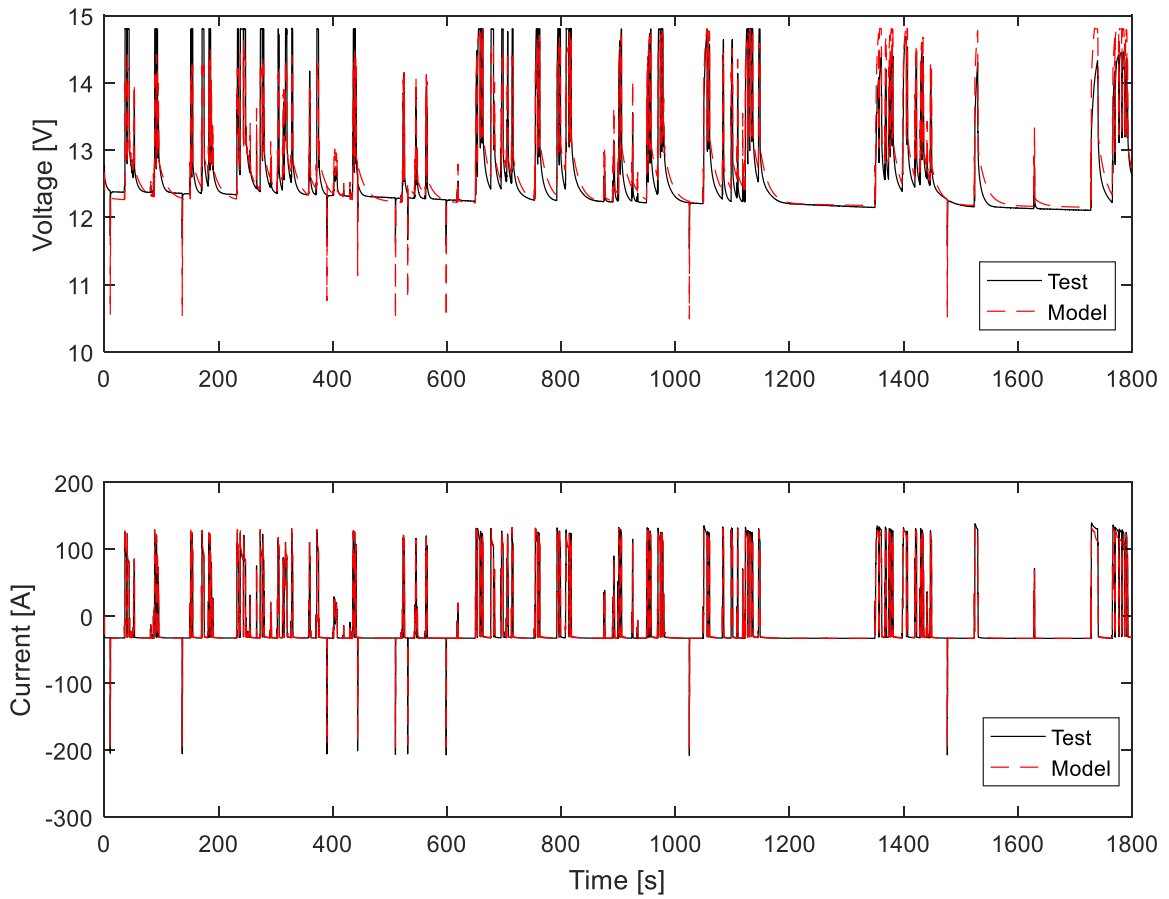


Figure 19: Baseline case fitting method for Modified Thevenin ECM of high load WLTP power profile (a) Measured vs. modeled voltage, (b) Measured vs. modeled current

Table 12: Summary of prediction accuracy for baseline fitting method of high load WLTP power profile using the Modified Thevenin ECM

<i>Performance</i>	<i>Max Error</i>	<i>Mean Error</i>	<i>RMS Error</i>
<i>Voltage [V]</i>	1.17	0.14	0.22
<i>Current [A]</i>	97.57	0.93	3.17
<i>Power [W]</i>	1387.57	4.80	37.16
<i>SOC [%]</i>	0.22	0.08	0.10
<i>Energy Throughput [Wh]</i>	1.70	1.27	0.33

The model performs as expected, though the voltage prediction is slightly worse on the higher load WLTP profile (where a greater number of constant voltage regions are incurred). The most concerning error is that using this model would result in an average of 1.27 Wh in energy throughput. This level of error could have implications on life predictions for batteries using this model.

4.2 Window Skip Algorithm

The second method which was considered was to simply ignore pulses which reach a voltage limit. This is done by scanning the profile for pulses which reach voltage limits

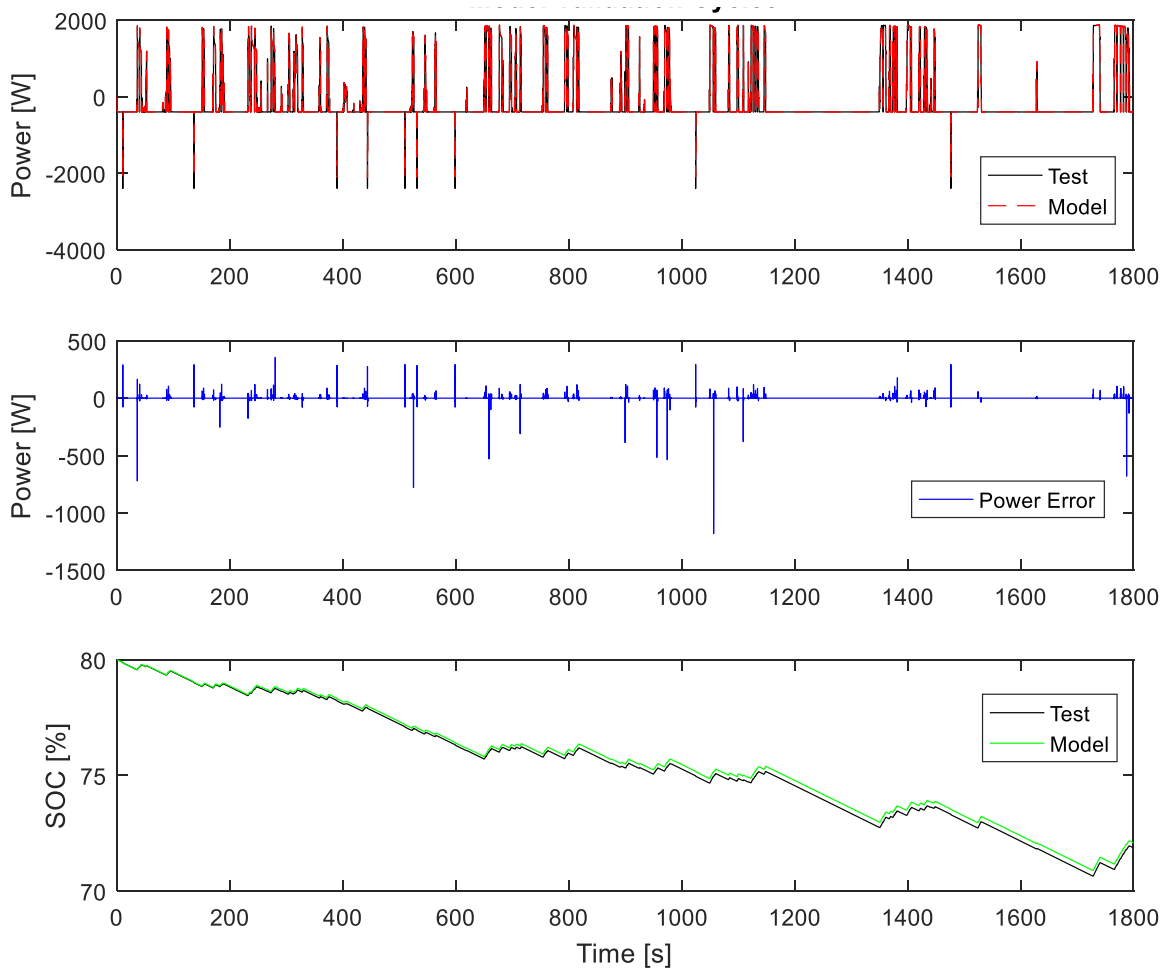


Figure 20: Window skip algorithm fitting method for Modified Thevenin ECM of high load WLTP power profile (a) Measured vs. predicted power, (b) Instantaneous, absolute error in power, (c) SOC calculated from test vs. modeled SOC

and omitting them from the fitting algorithm using the same logic shared in Figure 6. This method, while not highly sophisticated, was developed in order to reduce error in time constant estimation by limiting the amount of forced relaxation at a high voltage. While it was expected to under predict voltage in areas where a voltage limit is met, the hope was that the average battery behavior would be better described. The resulting predictions of the high load WLTP profiles are shown in Figure 20. and Figure 21 along with a statistical summary in Table 13.

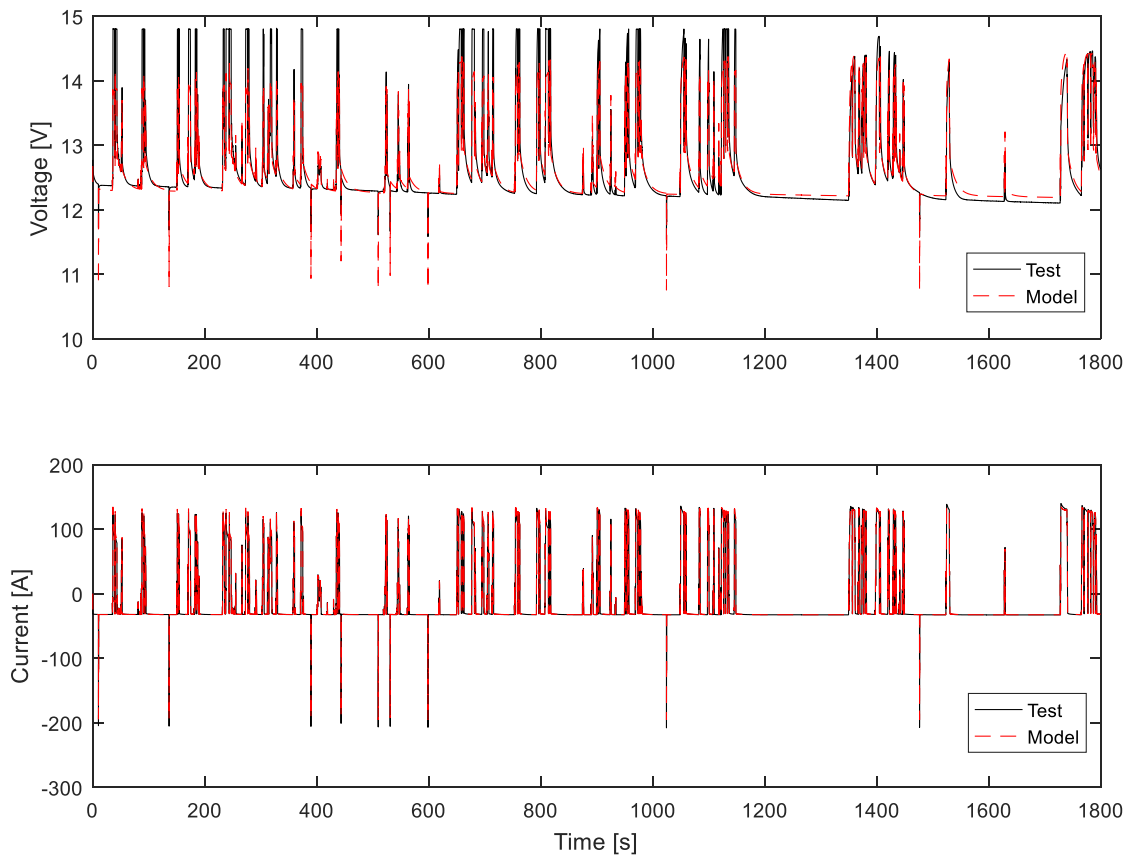


Figure 21: Window skip algorithm fitting method for Modified Thevenin ECM of high load WLTP power profile (a) Measured vs. modeled voltage, (b) Measured vs. modeled current

Table 13: Summary of prediction accuracy for window skip algorithm fitting method of high load WLTP power profile using the Modified Thevenin ECM

<i>Performance</i>	<i>Max Error</i>	<i>Mean Error</i>	<i>RMS Error</i>
<i>Voltage [V]</i>	1.05	0.11	0.20
<i>Current [A]</i>	84.95	0.61	1.92
<i>Power [W]</i>	1177.75	1.73	19.72
<i>SOC [%]</i>	0.20	0.12	0.13
<i>Energy Throughput [Wh]</i>	1.36	1.01	0.27

By skipping the voltage limited pulses, the model improves in the general accuracy of charging voltage predictions. By improving the charging voltage predictions, all key metrics are improved in their accuracy as well. Therefore, at the very least, voltage limits should be omitted from the dataset when conducting the fitting.

With that said, the behavior of the model under constant voltage charging is still lacking in accuracy. Depending on the actual application, this error could propagate to a level which might render the model useless. Therefore, one more method shall be considered for fitting datasets with voltage limiting cases.

4.3 Secondary Constant Voltage ECM

The final method introduces an additional equivalent circuit model. The secondary constant voltage ECM is designed so that it may predict the current, rather than the voltage, when the voltage is held constant.

The resulting model is a combination of two modified Thevenin ECMs which are switched on and off depending on the charge/discharge control variable.

This implementation requires an adjustment to the way in which current is calculated according to Figure 6. The new logic is outlined in Figure 22. By anticipating the constant voltage charge phases, a switch is made to the equivalent circuit model which was fit only using the constant voltage pulses.

Though this does add some complexity, the additional time required in generating the model and the subsequent validation require is negligible compared to the time required to generate additional test data.

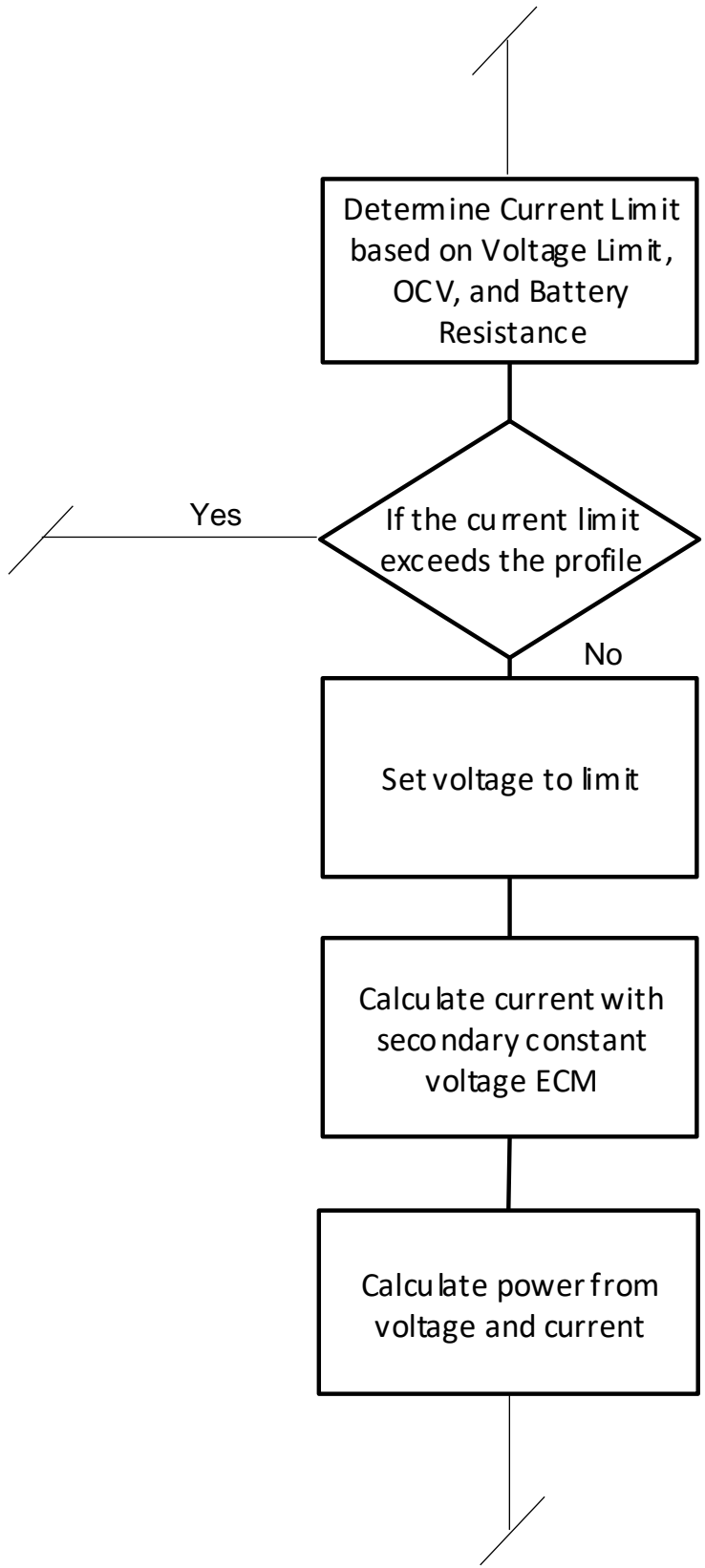


Figure 22: Modification of Figure 6. to include secondary ECM when the battery is in a state of constant voltage charging. Branches indicate a return to Figure 6.

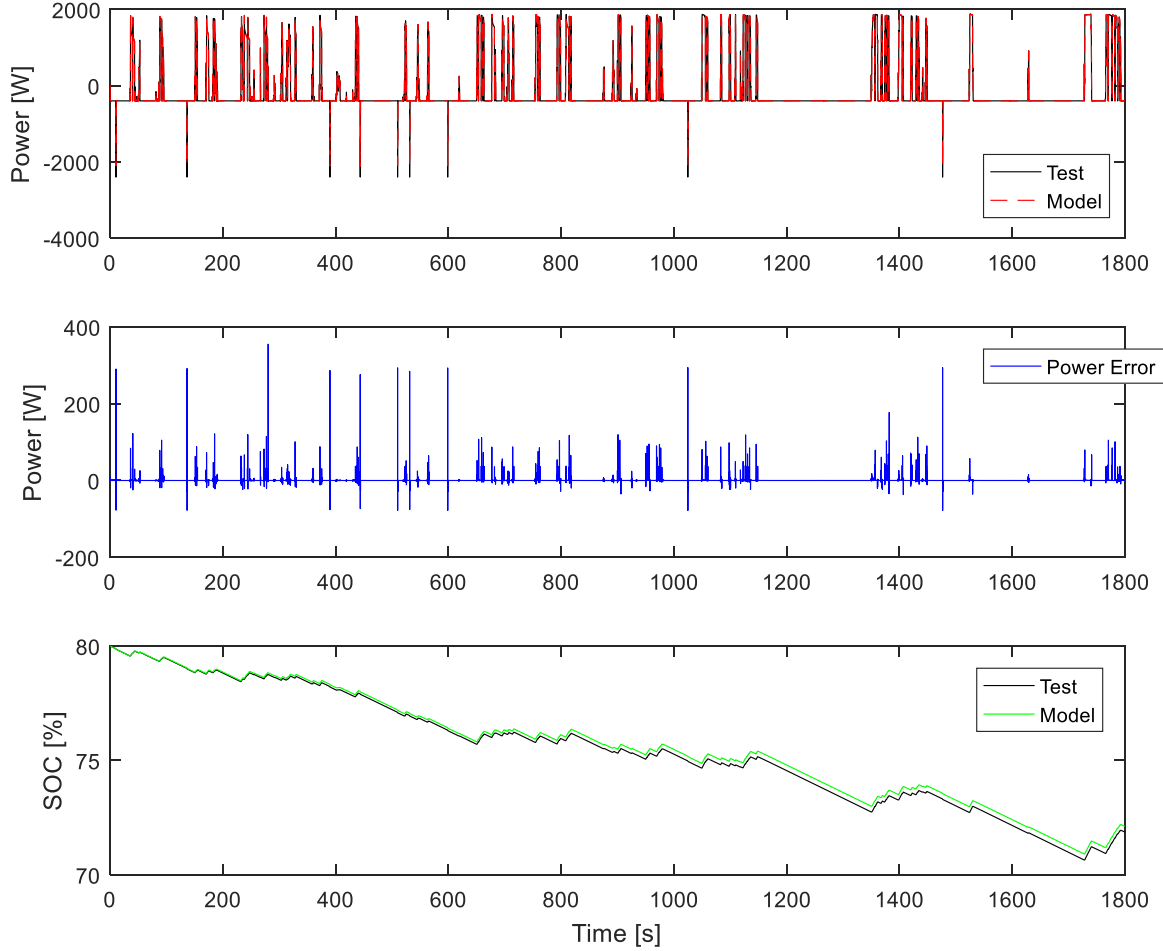


Figure 23: Secondary constant voltage ECM fitting method for Modified Thevenin ECM of high load WLTP power profile (a) Measured vs. predicted power, (b) Instantaneous, absolute error in power, (c) SOC calculated from test vs. modeled SOC

Fortunately, the implementation of this method yields the highest accuracy of those considered. The relative maximum error in power is reduced by 70% and the average energy throughput error is reduced by 56%. The voltage prediction is unaffected but the ability to model the current during constant voltage phases has a significant impact on the overall accuracy.

Table 14: Summary of prediction accuracy for secondary constant voltage ECM fitting method of high load WLTP power profile using the Modified Thevenin ECM

Performance	Max Error	Mean Error	RMS Error
Voltage [V]	1.05	0.11	0.20
Current [A]	27.45	0.58	1.44
Power [W]	357.25	1.31	9.91
SOC [%]	0.21	0.12	0.14
Energy Throughput [Wh]	0.46	0.44	0.11

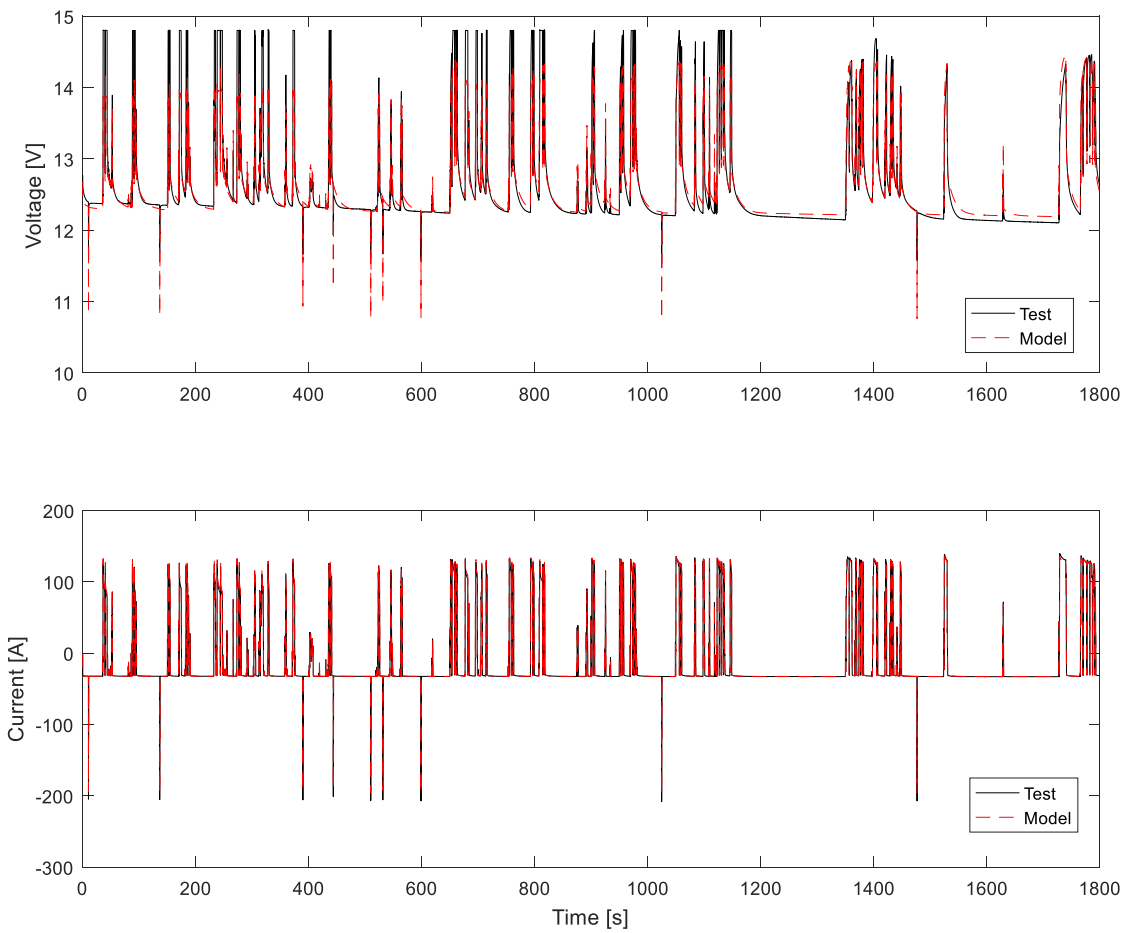


Figure 24: Secondary constant voltage ECM fitting method for Modified Thevenin ECM of high load WLTP power profile (a) Measured vs. modeled voltage, (b) Measured vs. modeled current

4.4 Conclusion

By assessing two separate methods for treating data with voltage limits, the accuracy of the fit was improved. When using the window algorithm to omit sections which incur voltage limited charging, the battery model is improved in accuracy across all measurements. By combining a model fit to only pulses controlled by current with a model fit to only pulses controlled by voltage, the power prediction accuracy is further improved. However, with this comes a slight increase in complexity and a small decrease in SOC accuracy (0.04% increase in average error). Therefore, depending on the desired optimization of the model, either the simple window algorithm or the additional voltage limited ECM should be used.

While both modifications increase prediction accuracy, it would be up to the engineer whether these provide a sufficient level of error for usage. For example, if the models are to be used to assess safety critical pulses, it is recommended to use a different characterization method or a higher accuracy model. However, for the purposes of general battery modeling and assessing performance within a vehicle, either fitting modification is considered sufficiently accurate.

By modifying the approach to fitting method, the accuracy was improved by ~70% in power prediction and ~56% in energy throughput prediction – two key output metrics from the battery modeling.

5. Conclusion

A total three equivalent circuit models were considered for both lithium ion and lead acid batteries. Lithium ion battery models were developed using HPPC data while lead acid battery models were developed using WLTP data. Though there are many differences between the two chemistries, they were shown to behave similarly by using the same set of equivalent circuit models.

As expected, an increase in accuracy was achieved by using a Thevenin model instead of a simple internal resistance model in both cases. Additionally, since the time constant was constrained by the constant voltage charging, an increase of accuracy was observed by using a modified Thevenin model which employs a different time constant on charge and discharge.

Constant voltage charging regions incurred when the battery meets its set limits negatively impacted the accuracy of the fit in all three models considered. By using a higher load profile which hit more voltage limits than the data used to develop the model, the ability to modify the fitting method to improve accuracy was assessed.

By fitting only pulses which did not hit voltage limits, the average fitting accuracy was improved in all metrics. Specifically, maximum power error was reduced from 1387 to 1177 W and average energy throughput error was reduced from 1.27 to 1.07 Wh.

Because this method is very simple, it might be recommended in areas where modeling accuracy isn't required in voltage limited scenarios. However, since the models are typically used for predicting battery behavior in driving applications, it was still desirable to improve the overall accuracy.

In the final section, an additional equivalent circuit model was employed to model the current during constant voltage phases (as opposed to modeling voltage). This model also employed an adjusted implementation to predict when voltage limits would be met in real-time. The secondary ECM for constant voltage charging led to a large increase in accuracy over the previous two methods. Specifically, the maximum power error was reduced from 1177 to 357 W and the average energy throughput error was reduced from 1.07 to 0.44 Wh. The one remaining drawback of this model implementation was slight increase from 0.08 to 0.12 % in average SOC error though this is small enough to be considered negligible.

Since the secondary ECM for constant voltage charging required negligible time to generate, it is considered the best method for predicting battery behavior when many constant voltage phases are present. In the case where few constant voltage phases exist, and the model is not expected to be used in these regions either, the window skip algorithm method would be a simpler and sufficient model.

While the inclusion of voltage limited regions requires some additional complexity in model development, it may not require a retesting of data. This is especially helpful when battery testing is developed to support vehicle applications such as the WLTP cycling.

REFERENCES

- 1) Richter, B.; Goldston, D.; Crabtree, G.; Glicksman, L.; Goldstein, D.; Greene, D.; Kammen, D.; Levine, M.; Lubell, M.; Savitz, M.; Sperling, D. *Energy Future: Think Efficiency*; American Physical Society: College Park, MD, 2008.
- 2) Johnson Controls expands AGM Battery portfolio to address increased electrification demands. (2017). *News Bites - Automotive*, pp. *News Bites - Automotive*, Nov 2, 2017.
- 3) The Global Lithium-ion Battery Market is set to Grow on Increasing Battery Applications. (2018). *PR Newswire*, p. *PR Newswire*, Oct 31, 2018.
- 4) Dubarry, & Liaw. (2007). Development of a universal modeling tool for rechargeable lithium batteries. *Journal of Power Sources*, 174(2), 856-860.
- 5) Salameh, Z., Casacca, M., & Lynch, W. (1992). A mathematical model for lead-acid batteries. *IEEE Transactions on Energy Conversion*, 7(1), 93,94,95,96,97,98.
- 6) Roscher, & Sauer. (2011). Dynamic electric behavior and open-circuit-voltage modeling of LiFePO₄-based lithium ion secondary batteries. *Journal of Power Sources*, 196(1), 331-336.
- 7) Jinxin Fan, Hongwen He, & Rui Xiong. (2011). Evaluation of Lithium-Ion Battery Equivalent Circuit Models for State of Charge Estimation by an Experimental Approach. *Energies*, 4(4), 582-598.
- 8) Chen, M., & Rincon-Mora, G. (2006). Accurate electrical battery model capable of predicting, runtime and I-V performance. *IEEE Transactions On Energy Conversion*, 21(2), 504-511.
- 9) Hu, Li, & Peng. (2011). A comparative study of equivalent circuit models for Li-ion batteries. *Journal of Power Sources*, 198(C), 359-367.
- 10) Guangming Liu, Lu, Hong Fu, Jianfeng Hua, Li, Ouyang, . . . Ping Chen. (2014). A comparative study of equivalent circuit models and enhanced equivalent circuit models of lithium-ion batteries with different model structures. *Transportation Electrification Asia-Pacific (ITEC Asia-Pacific)*, 2014 IEEE Conference and Expo, 1-6.
- 11) Lijun Zhang, Hui Peng, Zhansheng Ning, Zhongqiang Mu, & Changyan Sun. (2017). Comparative Research on RC Equivalent Circuit Models for Lithium-Ion Batteries of Electric Vehicles. *Applied Sciences*, 7(10), .
- 12) Buller, S., Thele, M., De Doncker, R., & Karden, E. (2005). Impedance-based simulation models of supercapacitors and Li-ion batteries for power electronic applications. *Industry Applications, IEEE Transactions on*, 41(3), 742-747.
- 13) Yannliaw, B. (2004). Modeling of lithium ion cells-A simple equivalent-circuit model approach. *Solid State Ionics*, 175(1-4), 835-839. doi:10.1016/j.ssi.2004.09.049

- 14) Demuynck, J., Bosteels, D., De Paepe, M., Favre, C., May, J., & Verhelst, S. (2012). Recommendations for the new WLTP cycle based on an analysis of vehicle emission measurements on NEDC and CADC. *Energy Policy*, 49(C), 234-242.
- 15) Worldwide Harmonised Light Vehicle Test Procedure. (n.d.). Retrieved from <http://wltpfacts.eu/>
- 16) Christopherson, J. P. (2015). *Battery Test Manual For Electric Vehicles, Revision 3*. Washington, D.C.: United States. Dept. of Energy. Office of Energy Efficiency and Renewable Energy.
- 17) Newman, J. (2010). *Electrochemical Systems*. Chicester: Wiley-Blackwell.
- 18) Tiedemann, W. (2008). Forty Years of Porous Electrode Theory with Battery Applications. *ECS Transactions*. doi:10.1149/1.2987756
- 19) Newman, J. S., & Tobias, C. W. (1962). Theoretical Analysis of Current Distribution in Porous Electrodes. *Journal of The Electrochemical Society*, 109(12), 1183. doi:10.1149/1.2425269
- 20) Chiasserini, C., & Rao, R. (2001). Energy efficient battery management. *Selected Areas in Communications, IEEE Journal on*, 19(7), 1235-1245.
- 21) Pascoe, P., & Anbuky, A. (2004). VRLA battery discharge reserve time estimation. *Power Electronics, IEEE Transactions on*, 19(6), 1515-1522.